UNIVERSITI PUTRA MALAYSIA

SURFACE PLASMON RESONANCE OPTICAL SENSOR FOR DETERMINATION OF CAFFEINE

HABIBUZZIKRI BIN AJEMAN

lp
FS 2022 24

SURFACE PLASMON RESONANCE OPTICAL SENSOR FOR DETERMINATION OF CAFFEINE

By

HABIBUZZIKRI BIN AJEMAN

195958

Thesis Submitted to the Department of Physics, Universiti Putra Malaysia, in partial Fulfilment of the Requirements for the Degree of Bachelor of Science in Instrumentation Science with Honours

January 2022

All material contained within the thesis, including without limitation text, logos, icons, photographs and all other artwork, is copyright material of Universiti Putra Malaysia unless otherwise stated. Use may be made of any material contained within the thesis for non-commercial purposes from the copyright holder. Commercial use of material may only be made with the express, prior, written permission of Universiti Putra Malaysia.

DEDICATION

To my beloved parents Ajeman Bin Jaimin and Salamah Binti Mohamed Sareh

For their unstoppable love and support

To my precious siblings and family

For their support and make my life full with happiness

To all my very cheerful friends

For the memories that we had been created together and make my life cheerful

To all my lectures

For helping me in this journey thoroughly and the knowledge given to me

Thank you all

© COPYRIGHT UPM

ABSTRACT

SURFACE PLASMON RESONANCE OPTICAL SENSOR FOR DETERMINATION OF CAFFEINE

By

HABIBUZZIKRI BIN AJEMAN 195958

January 2022

Supervisor: Assoc. Prof. Dr. Yap Wing Fen (PhD)

Department: Department of Physics, Faculty of Science.

Caffeine is one of the organic compounds that always have been used in food, beverages, powder, capsules and medicines. Caffeine consumption have many benefits such as increase alertness, easing fatigue and elevated blood pressure. Excessive caffeine intake can bring harm towards body. In this study, 3,5-diaminobenzoic acid (DIABA) and nanocellulose crystalline (NCC) has been used as sensing materials to detect caffeine using surface plasmon resonance (SPR) technique. Next, DIABA, NCC and DIABA/NCC thin film have been prepared by using spin coating technique at 5000 rev/min for 30 minutes. Gold thin film, gold thin film coated with DIABA and NCC separately found no change in resonance angle. It showed that no change for refractive index for all different caffeine concentrations. The used of gold modified by DIABA/NCC thin film with ratio 2:1 showed positive responses towards different caffeine concentrations as low as 0.5 nM. The SPR curves shifted to the left as the concentration increases. The sensor produced a linear response for caffeine with sensitivity of 0.05629 nM^{-1} and affinity constant value of

© COPYRIGHT UPM

0.6655 M^{-1}. The full width half maximum (FWHM) value was 2.96°, 2.99°, 3.04°, 3.05°, 3.06°, 3.04°, 3.02° and 3.21°. These produced the highest detection accuracy (DA) is 0.34/° at 0 nM and the lowest is 0.31/° at 100 nM. Thus, gold modified by DIABA/NCC thin film shows a good potential for detection of caffeine by using SPR.

© COPYRIGHT UPM

ABSTRAK

PENGESANAN KAFEIN MENGGUNAKAN SPEKTROSKOPI RESONANS PERMUKAAN PLASMON

Oleh

HABIBUZZIKRI BIN AJEMAN

195958

Januari 2022

Penyelia: Prof. Madya Dr. Yap Wing Fen (PhD)

Fakulti: Jabatan Fizik, Fakulti Sains

Kafein merupakan salah satu bahan organic yang sering digunakan dalam hidangan minuman, serbuk, kapsul dan ubat-ubatan. Pengambilan kafein mempunyai banyak kebaikan seperti meingkatkan kepekaan, mengurangkan penat dan tekanan darah tinggi. Pengambilan kafein yang berlebihan dapat mengundang keburukan pada badan. Dalam kajian ini, asid 3,5-diamino benzoik (DIABA) dan nanoselulosa kristal (NCC) digunakan sebagai bahan penderiaan untuk mengesan larutan kafein menggunakan teknik spektroskopi resonans permukaan plasmon (SPR). Filem nipis DIABA, NCC dan DIABA/NCC disediakan menggunakan teknik salutan spin pada 5000 putaran per minit untuk 30 minit. Filem nipis emas sahaja, emas disalut DIABA dan emas disalut NCC menunjukkan tiada perubahan pada sudut resonans. Ia menujukkan tiada perubahan pada indeks biasan pada setiap kepekatan kafein.

© COPYRIGHT UPM

Pengunaan filem nipis emas yang disalut DIABA/NCC dengan nisbah 2:1 menunjukkan tindak balas positif terhadap kepekatan kafein yang berbeza serendah 0.5 nM. Lengkungan SPR beralih semakin kekiri apabila semakin tinggi kepekatan. Sensor ini menunjukkan tindak balas linear terhadap kafein dengan nilai kepekaan 0.05629 nM^{-1} dan nilai pemalar pertalian 0.6655 M^{-1}. Nilai lebar penuh separuh maksimum (FWHM) adalah 2.96°, 2.99°, 3.04°, 3.05°, 3.06°, 3.04°, 3.02° and 3.21°. Ia menghasilkan nilai tertinggi ketepatan pengesanan (DA) ialah 0.34/° pada 0 nM dan terendah ialah 0.31/° pada 100 nM. Oleh itu, filem nipis emas disalut DIABA/NCC menunjukkan potensi yang bagus untuk mengesan kafein menggunakan SPR.

© COPYRIGHT UPM

ACKNOWLEDGMENT

First and foremost, I am very grateful to Allah the Almighty God for the wisdom he bestowed upon me, the strength, peace of mind and a healthy body to finish this research. I would like to give special thanks to my beloved parents, Ajeman Bin Jaimin and Salamah Binti Mohamed Sareh for having faith in myself and becoming one of the reasons for me to always do my best in my life. Not forget to my siblings for their love, encouragement, prayers and for always giving me mental support whenever I need.

I would like to express my special gratitude and give my warmest thanks to my supervisor, Assoc Prof. Dr Yap Wing Fen who made this work possible for giving me the opportunity to do research and providing invaluable guidance throughout this research. His continuous support and patience always inspired me to keep moving. I am highly indebted to all PhD and Master students in Applied Optic laboratory for sharing their knowledge and constructive suggestion to me in this project.

I would also like to thank my all lecturers and staffs in Universiti Putra Malaysia for that helped me in preparing the samples. Last but not least, my thanks and appreciations also go to my final year project teammates and my friends especially Muhammad Faris Zulkifli, Muhammad Nuwair, Aliuddin Anwar, Muhammad Amir Asyraf, Muhammad Hafiz Helmi and Abdul Rahman for mental support, cooperation and helped me a lot in process do this research. May Allah bless all of us.

© COPYRIGHT UPM

TABLE OF CONTENTS

© COPYRIGHT UPM

© COPYRIGHT UPM

LIST OF FIGURES

© COPYRIGHT UPM

© COPYRIGHT UPM

LIST OF TABLES

© COPYRIGHT UPM

LIST OF ABBREVIATIONS

SPR	Surface Plasmon Resonance
DIABA	3,5-Diaminobenzoic Acid
NCC	Nanocellulose Crystalline
LOD	Limit of Detection
FTIR	Fourier Transform Infrared Radiation
UV-Vis	Ultraviolet Visible
nM	Nanomolar
rpm	Revolution per minute
mL	Millilitres
nm	Nanometres
sec	Seconds

© COPYRIGHT UPM

CHAPTER 1
INTRODUCTION

1.1 Caffeine

Caffeine is the most abundant methylxanthine in foods. Caffeine (1,3,7-trimethylxanthine) one of organic compound from heterocyclic nitrogen atom with a purine base called xanthine, consisted of a pyrimidine ring linked to an imidazole ring. Caffeine also known as an alkaloid because it is a secondary plant metabolite derived from purine nucleotides (dePaula and Farah, 2019). The first chemical structure proposed by Ludwig Medicus (1847–1915) in 1875 which is deduced it from the already known pure compound. Then in 1882, Hermann Emil Fischer (1852–1919) was validating the caffeine and other methylxanthine structures. Nowadays, caffeine is one of the most popular drugs used in the food.

Caffeine is found in several commercial non-alcoholic beverages, powders, capsules and in association with therapeutic drugs to increased alertness. It is naturally found in food and beverages such as tea, coffee, chocolate, energy and colas. Caffeine consumption in daily life is an ancient habit. Moderate consumption this substance had effects of easing fatigue, increasing awareness, elevated blood pressure and alterations to mood. Energy drinks have also become attractive to teenagers and young adults worldwide. Caffeine is completely absorbed rapidly by human body and the effect can be seen within 15 to 30 minutes after consumption.

However, excessive caffeine intake can cause anxiety, headaches, nausea, restlessness, and an increase in the risk of hypertension and cardiovascular disease. The concentration of caffeine in the body is an important indicator for health. The consumption of caffeine is regarded to be harmless for adults (<100 mg/day). Then, the value suggested are 3 mg/kg

© COPYRIGHT UPM

per day for children and adolescents and maximum daily caffeine intake for pregnant women caffeine was set at 200 mg per day. Health Canada concluded that the general population of healthy adults is not at risk for potential adverse effects from caffeine at daily consumption levels up to 400 mg caffeine (Chen et al. 2019). A single high dose of caffeine (4–6 mg/kg equating to 300–400 mg for an average male) can cause abnormally rapid heartbeat and increased blood pressure. The risk of high blood pressure associated with coffee consumption may be higher in certain genotypes (Palatini et al, 2009).

1.2 Surface Plasmon Resonance

Surface plasmon resonance (SPR) is one of many optical methods for chemical sensing and biosensing that have been developed and used in the past. In the 1960s, Kretschman and Otto recognized the optical excitation of surface plasmons by attenuated absolute reflection in one of their SPR experiments. SPR sensor technology has been commercialized and SPR biosensors have become a central tool for characterizing and quantifying biomolecular interactions (Homola et al., 1999). Since then, the scientific community has been paying increasing attention to a variety of SPR sensing structures for chemical and biochemical sensing.

SPR is an optical process in which a monochromatic and p-polarized light beam hits an interface of two transparent media from the side of the media with a higher refractive index (glass prism), the light is partly reflected and partly refracted towards the plane of the interference (Fen and Yunus, 2013). Then, above a certain incidence angle, none of the light is refracted and the phenomenon is called total internal reflection. Then, it excites a charge-density-wave propagating along with the interface between a metal and a dielectric material. Because of the resonance between the incident beam and the surface plasmon wave, the

© COPYRIGHT UPM

intensity of the reflected light is reduced at a specific incident angle, resulting in a sharp shadow. This phenomenon is called SPR.

There are some detections approached in SPR which are prism coupler-based SPR sensor, grating coupler-based SPR sensor and optical fiber-based SPR. These different techniques are approached depending on the target senses. In wavelength interrogation mode for grating-based optical SPR sensors, a high-sensitivity SPR grating-based gas sensor using silver as an SPR active metal achieved a sensitivity of 1000 nm RIU^{-1}; in angular interrogation mode, the system's sensitivity would be about 100 degrees RIU^{-1}. By multiples of the grating wave vector, the portion of momentum of these diffracted beams along the interface varies from that of the incident wave. The optical wave can couple to the surface plasmon wave (SPW) if the total component of momentum along the interface of a diffracted order is equal to that of the SPW. The mathematics involved in modeling grating SPR-sensing systems is more complicated, and it is more difficult to model the structures and analyses sensor data (Homola et al., 1999).

Jorgenson and Yee were the first to consider in 1993 using optical fibers for SPR sensing. They used a traditional polymer clad silica fiber with partly removed cladding and an SPR active metal layer deposited symmetrically around the exposed portion of the fiber core to create an SPR-sensing structure. With a resonant wavelength resolution of 0.5 nm, a fiber optic SPR sensor can detect variations in refractive index within the operating range of 1.2 and 1.4 RIU with a resolution of up to 5×10^{-5} RIU^{-1} at higher refractive indices of the analyte. Both types of multimode fiber optic SPR-sensing systems have a low level of stability in general. Mechanical disruptions close to the sensing region of the fiber can trigger intermodal coupling and modal noise because the modal distribution of light in the fiber is very sensitive to them. The operating range of single-mode fiber SPR sensors is, of course, extremely small. A high refractive index dielectric overlayer can effectively tune the sensor's

© COPYRIGHT UPM

operating range; however, the presence of the dielectric overlayer can reduce the sensor's sensitivity.

In this case, the prism coupler which has higher sensitivity of SPR sensors by using ATR prism couplers than the SPR devices based on grating couplers. The Kretschmann geometry of the ATR system, in particular, is particularly well suited to sensing and has become the most commonly used geometry in SPR sensors. A light wave is totally reflected at the interface between a prism coupler and a thin metal layer (around 50 nm thickness) and excites an SPW at the metal's outer boundary by evanescently tunnelling through the thin metal layer in this configuration. In SPR prism-based sensors, all of the major detection approaches have been demonstrated; measurement of the reflected light wave's intensity, measurement of the light wave's resonant angle of incidence and incident light wave's resonant wavelength. It was possible to achieve a refractive index resolution of better than 3×10^{-7} RIU^{-1}. Using silver as the SPR active medium, an earlier wavelength interrogation-based SPR sensor achieved a sensitivity of around 3200 nm RIU^{-1}, compensating for activity in the low sensitivity spectral area around 640 nm. In terms of the analyte refractive index covered, bulk prism-based SPR devices offer a lot of versatility. High-quality bulk optics enable the production of SPR systems with low optical noise, allowing for high-resolution measurements (Homola et al., 1999).

The sensing operation is performed directly in the region where the SPW is excited by an optical wave due to the short propagation duration of SPW. The optical system used to excite the SPW is also used to interrogate the SPR. As a result, increasing the sensor's contact length, as is usual in sensors using directed modes of dielectric waveguides, will not improve the sensitivity of SPR sensors. The Kretschmann configuration was used in the majority of SPR applications, where a metal film, usually gold or silver, was positioned at the interface of two dielectric media. SPR occurs when plane-polarized light collides with a thin metal

© COPYRIGHT UPM

film under complete internal reflection conditions. After that, the reflected beam will be detected and processed. Optical sensing is one of the most popular applications for SPR that are employed in a variety of sectors, including food safety, environmental safety, and disease detection (Özgür et al., 2020).

The sensitivity of SPR sensors has been extensively researched. The sensitivity of SPR angular interrogation-based sensors to changes in the refractive index increases as the activity wavelength decreases, while the sensitivity of SPR refractive index sensors using wave-length interrogation and intensity calculation increases as the wavelength decreases (Homola et al.,1999). In the experiment, sensing material (3,5-Diaminobenzoic Acid and Nanocellulose Crystalline) will be introduced as the active layer on the thin film. This action will increase the refractive index and also will increase the sensitivity to detect the caffeine.

1.3 3,5-Diaminobenzoic Acid and Nanocrystalline Cellulose

In present study, 3,5-diaminobenzoic acid (DIABA) was enzymatically polymerized with HRP enzyme in organic solvent phosphate tampon solution (pH 7) using hydrogen peroxide (H_2O_2) as an oxidant. H_2O_2 oxidant was used to establish DIABA oxidative polymerization in an aqueous simple medium at 70°C. Besides, the fluorescent probe DIABA was used to detect the caffeine aqueous solution. Caffeine does not have any fluorescence properties, but DIABA does. A previous study discovered a noncovalent interaction between caffeine and DIABA that resulted in DIABA fluorescence quenching (Du et al., 2020). A simple, efficient, low-cost fluorescent probe was developed based on the fluorescence quenching effect of caffeine on DIABA. The high selectivity of DIABA for caffeine has been demonstrated.

© COPYRIGHT UPM

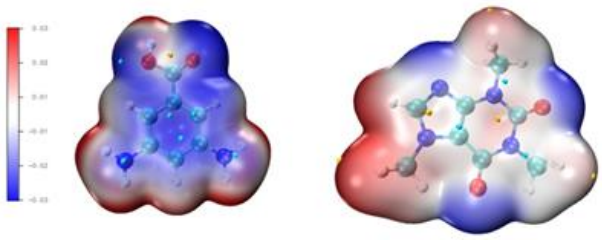

(a) **(b)**

Figure 1.1: The molecular electrostatic potential of 3,5-diaminobenzoic acid and caffeine.

The interactions between caffeine and DIABA are explained using the electrostatic potential of surface molecules. The negative potential of the molecule is represented by the blue regions, while the positive potential is represented by the red regions. The potential near the benzene ring in DIABA is negative, whereas the potential near the carbon atom in caffeine is positive, indicating that these two molecules shape the caffeine-DIABA complex more easily, as shown in Figure 1a, b. We also discovered that the potential near the oxygen atom in DIABA is negative, suggesting that this atom is more likely to absorb free protons, while the potential near the hydrogen atom in caffeine is positive, indicating that the two are very simple to combine (Du et al., 2020).

Sulfuric acid catalyzed the degradation of cellulose in the first study on the development of nanocellulose crystalline (NCC) from native and mercerized wood cellulose, as well as viscose rayon, published in 1950. The broad surface area for presenting hydroxyl groups is inhibited when NCC is generated in an acidic environment. NCC comes from a variety of sources such as wood, flax, bacterial cellulose, tunicate, and microcrystalline cellulose (MCC). There are various methods for the preparation of these crystalline nanoparticles depending on the type of cellulose raw materials, their pretreatment and their decomposition process. The most common method is hydrolysis by acid. NCC has significant properties, including high tensile strength, high hardness, broad surface area, low

© COPYRIGHT UPM

density, high aspect ratio, changeable surface properties due to hydroxyl reactive groups, and other electrical, mechanical, thermal, and optical properties, as one of the strongest and stiffest natural materials available. NCC has significant properties, including high tensile strength, high hardness, broad surface area, low density, high aspect ratio, changeable surface properties due to hydroxyl reactive groups, and other electrical, mechanical, thermal, and optical properties, as one of the strongest and stiffest natural materials available (Karimian et al., 2019).

1.4 Problems Statement

The detection of excessive caffeine is very important due to their bad effects on human body system as mentioned earlier. Lots of studies have been conducted to detect the caffeine. Various method have been used to determine caffeine in samples of different teas and beverages such as high-performance liquid chromatography (HPLC), gas chromatography-mass spectrometry (GC-MS), high performance liquid chromatography-mass spectrometry (HPLC-MS), electrophoresis, capillary electrophoresis (CE), high performance thin layer chromatography (HPTLC), UV-visible spectrophotometry, voltammetry, micellar liquid chromatography, ion mobility spectrometry and fluorescence sensing (Du et al., 2020).

However, most of these techniques requires massive amount of time, laborious and costly. In addition, these methods also need to do pre-processing which might increase the possibility of error in the research and experiment. Therefore, SPR has been selected in this study to determine the caffeine. Although it has been around for 20 years, yet many researchers still rely on it to characterize biological interactions because of affordable and accessible (Nguyen et al., 2015). The ability to test the interaction between the analyte and ligand without wasting time and resources on costly labelling reagents and protocols is one of the key features of the SPR. It also requires minimal amounts of sample for binding

© COPYRIGHT UPM

kinetics experiments. This means having to express, purchase, and purify less sample than other techniques. The interaction can be described by examine what happens in real time. This information is provided by SPR, which reveals more than just the tip of the iceberg by offering greater insight. SPR also has a number of benefits, including being cost-effective, requiring only basic sample preparations, being able to measure easily, and not requiring the use of a reference solution (Fen et al., 2012). However, the SPR technique for caffeine detection, there were limited work been done.

In addition, most of the studies have low sensitivity detection of the caffeine. This might be a problem to detect the existence of caffeine at the lowest concentration. The determination of caffeine is important at low concentration due to the effect of its consumption. Active layer is one of the efforts to enhance the sensitivity in determination of target material by using SPR. There is still no study in determination of caffeine using DIABA and NCC as the sensing material. By adding the active layer as sensing material might be increase the sensitivity and detection range in SPR (Fen et al., 2012). Hence, this is new approach of the SPR in attempting by using DIABA and NCC based for sensing the determination of caffeine.

1.5 Research Objectives

The objectives of this work are:

i. To study the detection of caffeine by using surface plasmon resonance (SPR) method.
ii. To analyze the performance of SPR sensor in caffeine detection using 3,5-diaminobenzoic acid (DIABA) and nanocellulose crystalline (NCC) as sensing elements.

© COPYRIGHT UPM

CHAPTER 2

LITERATURE REVIEW

2.1 Optical Technique for Determination of Caffeine

In the beginning of sensing and detection era, there are many techniques that have been developed by the researchers. Currently, optical sensors are one of the most established techniques to determine chemical analytes, metal ions, and enzymatic analytes makes researchers' interest in further developing the technology for advanced technologies. Optical biosensor has provided a good performance in diagnosing for high selectivity and sensitivity, rapid detection and handling facilities (Omar et al., 2019). The example of optical methods that widely used are colorimetric, surface-enhanced Raman spectrometry, electrochemiluminescence, chemiluminescence, fluorescence, photoelectrochemical, spectrophotometric, photoluminescence and UV-Vis. Until now, various types of material and optical techniques have been developed, in order to increase the sensitivity and also the selectivity for detecting caffeine.

In 1953, Goldbarg has developed an experiment for caffeine detection by using colorimetric method. The reported the detection limit was 440.00 μM which applied to sample containing 1 to 5 mg. In 1995, Amin and El-Henawee have detected anhydrous caffeine by using colorimetric method in dosage forms. Rose bengal has been used as a sensing material. It was obeyed in the concentration ranges 10.30-175.10 μM. Meanwhile in 2007, Kim et al. used colorimetric method in rapid screening of low-caffeine-containing tea (Camellia synesis) trees by using ethyl acetate. The result showed that the caffeine was in the range of concentration from 0.92-4.40 mM. Next, Deng et al. used silver nanoparticles

© COPYRIGHT UPM

(AgNPs) as sensing materials in colorimetric. The limit of detection was 5.15 μM for the detection range of 0.52-25.75 μM.

In 2006, there was another study in caffeine detection by using fluorescence method. Siering et al., in 2006 were carried out an experiment by using methanol at a constant temperature of 25 °C. After correction for offsets, standard deviations reported were smaller than 2 percent in caffeine concentration of 5.00-50.00 μM. In 2011, Rochat et al. used 8-hydroxypyrene-1,3,6-trisulfonate (HPTS) as fluorescent sensing material to make π-stacking interactions with caffeine. The study has showed the detection limit was 170.00 μM. Furthermore in 2012, Luisier et al. used another molecular probe which is disodium 3,4:3′,4′-bibenzo[b]thiophene-2,2′-disulfonate in fluorescence to detect caffeine in aqueous solution. The detection range reported from the experiment was 0-7.50 mM.

Moreover, Ghosh et al. (2013) used another approach in fluorescence by using acridine orange (AO) as a sensing probe to create selective and sensitive caffeine determination in aqueous solution. Caffeine's interaction with AO monomer causes a change in the AO dimer monomer equilibrium in favor of AO monomer (fluorophore). Lowest detection reported in this study was 100 μM in the range detection between 15−25 mg/g. The next two years, Gliszczyńska-Świgło and Rybicka used fluorescence approach with methanol as a sensing substance in detection of caffeine. They found the lowest detection for caffeine was 118.44 nM in the range of 0 to 2.58 μM. Besides, Nanjundaiah et al. in 2016 developed a study in caffeine detection using europium-tetracycline as sensing material by the same method. Overall, the detection limit highlighted in the research was 51.50 μM with the detection range between 0.052 to 51.50 mM.

In 2016, Xu and Chang reported a study caffeine detection by fluorescence using two different sensing materials which are 8-hydroxypyrene-1,3,6-tri-sulfonate (HPTS) and Acridine Orange. The π-stacks between HPTS and caffeine were shown to be responsible

© COPYRIGHT UPM

for their association and subsequent fluorescence quenching in computational research. The interaction between AO monomer and caffeine is π-stacking pattern might be utilised to determine caffeine levels in commercial tea samples. In 2018, Nemati et al. demonstrated a fluorescent probe of sulphur-doped carbon quantum dots (S-CQDs) to detect caffeine. Under 365 nm UV light stimulation, the produced S-CQDs produced intense blue fluorescence with a high quantum yield of 21.4 percent. The detection limit reported was 0.05 μM in detection range between 0.20 and 70.00 μM. Lastly in 2020, González et al. and co-workers used fluorescence method for caffeine detection in beverage samples by using glibenclamide (GLB). GLB has a strong emission at 350 nm, with an excitation maximum at 234 nm and 298 nm. The lowest detection limit of caffeine was found to be 0.52 μM.

On the other hand, another optical technique which widely used to detect caffeine is surface-enhanced Raman spectrometry. In 2014, Hughes et al. used 1.3 nm silica-coated nanoparticles as the sensing material to detect caffeine. The result showed lowest caffeine concentration found was 1.00 μM approximately. In 2015, Franzen et al. developed an experiment to detect caffeine by surface-enhanced Raman spectrometry approach. Buffer, phosphoric-acid, potassium-dihydrogen phosphate has been used as sensing materials. The study reported limit of detection was 2.50 μM in the range between 0.50 μM and 30.00 μM. Then, Zheng et al. have developed silver nitrate ($AgNO_3$) as a sensing material in surface-enhanced Raman spectrometry. By using this approach, the lowest detection shown was 1.00 nM. Next in 2020, de Souza et al. has applied surface-enhanced Raman spectrometry for caffeine detection. In this study, citrate, borohydride, hydroxylamine and β-cyclodextrin silver sols were chosen as a sensing material. The detection limit highlighted in this experiment was 0.10 mM.

Besides, photoluminescence is another optical method for caffeine detection. Masoum and Heshmat in 2019 used phosphate buffer solution as the sensing material to detect

© COPYRIGHT UPM

caffeine in green tea. As the result, the caffeine detection range in this experiment was 15.45 to 66.94 μM. Another method which are widely used in caffeine determination was spectrophotometric. In 1999, Luque-Pérez et al. developed an approach in caffeine detection using spectrophotometric with PTFE-undecane: hexylether as the sensing material. The limit of detection that has been reported was 2.06 mM with the detection range 2.58-77.24 mM. After 3 years, the research in caffeine determination is still growing. Spectrophotometric has been used in 2002 by Ferreyra and Ortiz in caffeine detection by using 3,7-dihydro-1,3,7-trimethyl-1 H-purine-2,6-dione as the sensing material. The detection range that has been reported was 12-28 μM with the lowest detection limit of 1.48 mM.

Moreover, Amos-Tautua et al. (2014) have conducted an experiment using spectrophotometric method for caffeine detection. Carbon tetrachloride have been used as the sensing materials. The detection limit reported was 10.09 μM with the range of the detection between 10.30-164.80 μM. Next, by using similar method, Xia et al. (2012) have integrated different sensing material which is cerium sulphate in sulphuric acid. They reported the lowest detection caffeine was 1.55 μM for the detection range between 2.06 to 43.26 μM. Meanwhile in 2015, Ahmad Bhawani et al. managed an experiment using spectrophotometric to detect caffeine in various medicines. The result showed limit of detection was 20.6 μM with the detection range between 5.15 and 128.74 μM. Last but not least in 2021, Ogunneye et al. used dichloromethane and hydrochloric as the sensing material in spectrophotometric method. The lowest detection reported in the range of 5.15-128.74 μM was 0.9887 μM.

© COPYRIGHT UPM

2.2 Sensing Properties of 3,5-Diaminobenzoic Acid

Recently, there are many types of sensing materials have that been developed around the world which created from different kind of reactions to detect caffeine. 3,5-diaminobenzoic acid (DIABA) already known as one of the most promising conductive organic materials. The chemical and physical properties and characteristics of DIABA has been greatly influenced by the presence of carboxyl and amine groups (Tang and Wang, 2020). In 2020, Du et al. reported that the caffeine's quenching intensity for DIABA is substantially higher than other interfering materials, which proves its high selectivity to caffeine. The small amount of DIABA was used to optimized the reaction conditions (Thomas and Farquhar, 1997). This shows that DIABA could be one of the factors to lower cost, high sensitivity, fast detection in the experiment and suitable to use in caffeine detection.

Firstly, Du et al. in 2020 used DIABA as sensing materials for detect caffeine. The experiment was carried out by using fluorescence method. Under the excitation of light at 280 nm, the DIABA displays intense fluorescence about 410 nm. A good linear correlation was obtained in the detection range from 0.1-100 µM with a limit detection of 0.03 µM. In the next year, Gong et al. in 2021 developed a research to determine hydrogen sulfide which the typical metabolic marker in body. They used the DIABA as the functional monomer to modify on the CAU-10-NH_2. During the 412 nm under an excitation wavelength of 320 nm, the NH-dAba has strong fluorescent performance. The experiment recorded a linearity range between 0.02-0.14 µM with detection limit of 1.51 nM.

Lastly, besides a detecting caffeine and hydrogen sulfide, Gamonchuang and Burakham managed to detect phenol in 2021 by using DIABA via magnetic solid phase extraction method. The presence of amino groups on the sorbent allowed for effective interactions amongst the phenol compounds. The results obtained in the concentration in the

© COPYRIGHT UPM

range of 2.575 to 5.15 µM depends on compound. The detection limits varied from 51.5 pM to 1.545 nM.

2.3 Sensing Properties of Cellulose

In recent decades, there are many sensing materials that has been used in detection by optical sensors. Cellulose is a chain of glucose that easily obtained from nature as known as most common natural polymer. Cellulose that prepared from plant usually used in engineering properties preferred for mass production due to the cost effectiveness. In terms of fundamental properties, cellulose displayed remarkable stiffness, strength, and thermal stability. In several areas of application, cellulose and cellulose-based composites have improved and grown during the last three decades. It was really encouraging to be able to add value to cellulose for any potential use from the aspect of a sustainable and renewable material (Ummartyotin and Manuspiya, 2013).

In 2020, an experiment have been developed by Shehata et al. to detect caffeine by using electrochemical method. The research has carried out using cellulose acetate. The development of a novel electrodeposited Ag nanoparticles-cellulose acetate phthalate (CAP)-chitosan (Chit) modified carbon paste (ACCMCP) sensor for sensitive determination caffeine of 0.01 mol L^{-1}. Caffeine had a linear detection range of 4 to 500 µM L^{-1} and the calibration plot revealed that the limit of detection was 0.25 µM L^{-1}. Moreover in 2005, Zhang et al. used cellulose acetate filter, borate solution and methanol in the electrophoresis with electrochemical detection experiment. Caffeine and theophylline were successfully determined in rat serum and urine by using the suggested approach. The detection limit was 4.00 µM in the range of caffeine concentration from 6.00 µM to 0.60 mM. In the same year, Huck et al. (2005) have compared the potential of cellulose filter by using infrared spectroscopy (NIRS) and high-performance liquid chromatography (HPLC)

© COPYRIGHT UPM

coupled to mass spectrometry methods. The lower limit of detection for NIRS method is found at 0.05 g/100 g compared to LC method which is 0.244-0.60 ng/100g (LC) in a concentration range between 0.10 and 4.13 g/100 g.

2.4 SPR for Caffeine Determination

Surface plasmon resonance (SPR) is a well-known as one of optical sensing method. Liedberg et al. described the first application of the SPR method for sensing in 1983. Since then, a rising number of SPR sensing structures for chemical and biochemical sensing have attracted the attention of the scientific world.

In 2009, Roche et al. developed analysis of caffeine binding to Cytochrome p450 monooxygenases in the presence and absence of NADPH based on surface plasmon resonance technique. In their work, they obtained high sensitivity results which recorded in the range between 0.05 to 0.175 M. After that in 2017, Kant et al. integrating nanohybrid membranes of reduced graphene oxide, chitosan and silica sol gel with fiber optic surface plasmon resonance method for caffeine detection. The lowest detection recorded was 1.994 nM in the range of 0-0.5 µM concentration. Moreover, Yekta et al. (2021) reported an interaction of caffeine on tau-tau proteins based on localized surface plasmon resonance detection. The limit of detection of 0.5 µM in the range of detection between 0-20 µM.

© COPYRIGHT UPM

CHAPTER 3

METHODOLOGY

3.1 Surface Plasmon Resonance

3.1.1 Basic Principle

Surface plasmon resonance (SPR) sensor is a physical phenomenon that occurs when polarised light is projected through a prism coated with a thin gold sensor surface (Kretschmann's arrangement), the energy is transmitted to the electron of metal which are transformed into surface plasmons at the interface. Under a specific incidence angle, all incoming light is reflected. This phenomenon known as total internal reflection. While the incident light is completely reflected, the electromagnetic field component travels through the gold for a short distance.

SPR is a method for detecting changes in the refractive index of a sensor's surface which is actually a glass coated with a thin film. A light beam will partially reflect and partially refracted as it travels through a surface with a different refractive index. Then, total internal reflection happens since the incident angle of light is greater than critical angle and no light will be refracted. The total internal reflection that occurs at the prism-metal interface when the angle of incidence of the beam is larger than the critical angle produces the evanescent wave required to excite surface plasmons in the case of a prism-based SPR sensor (Gupta and Verma, 2009).

© COPYRIGHT UPM

3.1.2 Experiment Setup

3.1.2.1 Laser

The light source that was used in SPR technique is Helium-Neon (He-NE) laser. Helium-neon (He-Ne) lasers as shown in Figure 3.1 are widely used for interferometry because they are inexpensive and provide a continuous, visible output. In this study, wavelength that have been used to operate was 632.8 nm. The light source went through the chopper, polarizer and hit the prism.

Figure 3.1: He-Ne laser used as source of light.

3.1.2.2 Chopper

The optical chopper as shown in Figure 3.2 that has been used was SR540. The device is used to interrupt the light laser. Three types of choppers are rotating disc choppers, fixed frequency tuning fork choppers and also optical shutters (George et al., 2015). In this study, the intensity of light beam from He-Ne laser will be modulated by using rotating disk chopper. The light beam is disrupted (chopped) at regular intervals when the disc rotates at a certain frequency. The interval at which the beam is chopped will be determined by the nature of the slots on the disc and the frequency of rotation.

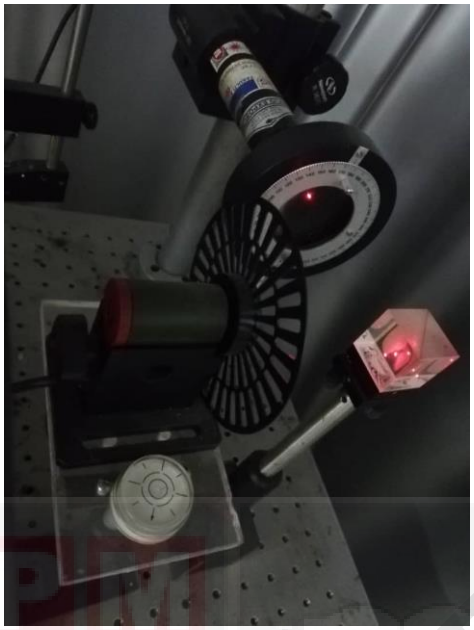

Figure 3.2: Example of chopper used for SPR sensor.

3.1.2.3 Polarizer

A polarizer as shown in Figure 3.3 is a device that turn unpolarized light into polarized light by selective absorption, refraction or transmission. A linear polarizer's basic function is to absorb, scatter, or reflect light in the unwanted polarization direction. Only one polarization state may be transmitted by linear polarizers. The device is oriented at 90 degrees to each other by transmitting and absorbing axes. After the unpolarized light which travels in random direction, travels through the linear polarizer, it has an electric field in one direction and may be considered as a linear combination of two vectors with the same phase (vertical and horizontal) (Lin et al., 2000). In this study, p-polarized light will be used because the electric field is parallel to the plane of incidence, while perpendicular (s-) polarization is when the electric field is perpendicular to the plane of incidence.

© COPYRIGHT UPM

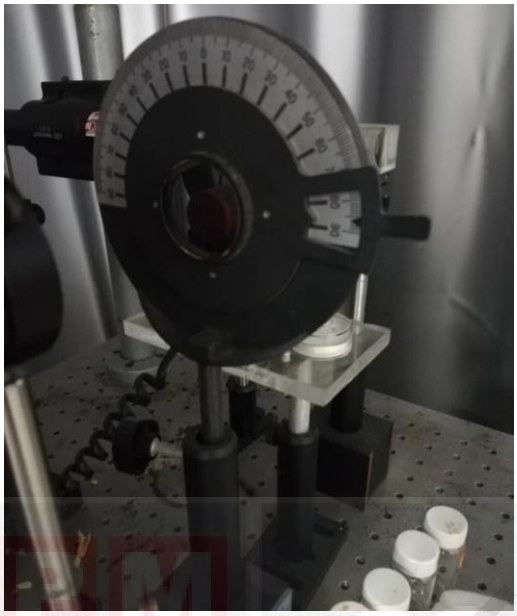

Figure 3.3: Unpolarized light will travel through polarizer.

3.1.2.4 Stage

Optical stage will be used to record the signal from the laser for every angle. The angle will be controlled by optical stage. The optical stage was driven by a stepper motor. The prism based on kretchmann configuration and the hollow cell were placed on the rotating plate on the stage to control the angle of incident light. To perform the SPR measurement, the prism was put on an optical stage as shown in Figure 3.4 powered by a stepper motor with a precision of 0.001 (Newport MM 3000).

© COPYRIGHT UPM

Figure 3.4: Prism placed on an optical stage.

3.1.2.5 Photodiode

A photodiode as shown in Figure 3.5 is a p-n junction semiconductor device that transforms light into electricity. A wide area of photodiode detected the reflected beam, which was then processed by the photodiode and transferred to the lock-in amplifier. To detect light, photodiodes employ a junction between p-type and n-type semiconductors. An n-type semiconductor has a lot of highly mobile electrons, while a p-type semiconductor has fewer highly mobile positive holes. In this study, p-n junction was used. The reflected light is processed by photodiode.

© COPYRIGHT UPM

Figure 3.5: Photodiode used to detect the reflected light.

3.1.2.6 Motor Controller

A stepper motor is used in conjunction with digital control to produce accurate positioning. The motor as shown in Figure 3.6 runs by precisely synchronising with the controller's pulse signal to the driver. Stepper motors are suitable for applications that need fast positioning over a small distance due to their ability to provide strong torque at a low speed while reducing vibration. The stages may be operated simply from a PC via a graphical user interface (GUI) that allows the user to interact with the controller, which is combined with intelligent stepper motor stages. Basic motion, changing the status of the controller, adjusting configuration parameters, and developing sophisticated application programmes are all possible using the GUI. It rotates at fixed step angle known as “basic step angle” which are 0.36°, 0.72°, 0.9°. 5-Phase stepper motors provide 0.36° and 0.72°, while 0.9° and 1.8° step angles offered by 2-phase stepper motor.

© COPYRIGHT UPM

Figure 3.6: Angle of rotation controlled by motor controller.

3.1.2.7 Lock-in Amplifier

The function of lock-in amplifier is to detect and measure very small AC signals as low a few nanovolts. The small signal can be obscured thousands of times larger by noise sources. To separate the component of the signal at a given reference frequency and phase, lock-in amplifiers apply a method called as phase-sensitive detection. In this study, we will use lock-in amplifier (SR540) as shown in Figure 3.7.

Figure 3.7: Example of lock-in amplifier used in SPR setup.

© COPYRIGHT UPM

3.1.2.8 Prism and Cell

The most important part in this technique is setup for the excitation of surface plasmons using Kretchmann configuration by prism and cell as shown in Figure 3.8. In this configuration, glass prism with dimension of 24 × 24 mm and thickness of 0.13-0.16 mm that was purchased from Menzel-Glaser was coated by a thin layer of gold (thickness = 50 nm). Gold have been used as metal film to be placed at the interface between two dielectric media. In this study, gold was used because gold contain electrons in the conduction band that can resonate with incoming light at an appropriate wavelength. It must be devoid of oxides and sulphides, and it must not react with other molecules when exposed to air or water. The gold was deposited using sputter coater machine (SC7640) at 67 sec to achieve 50 nm thickness. The gold thin film will be placed on glass prism with refractive index of 1.7786. Then deionized water and caffeine solution with different concentrations was injected into the dielectric media one by one for ten minutes before the signal was recorded. The schematic diagram of complete SPR setup designed in the laboratory is shown in Figure 3.9.

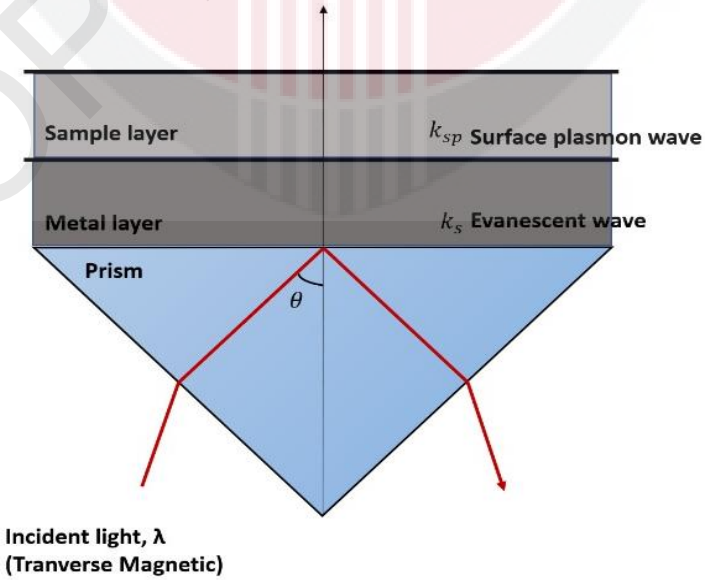

Figure 3.8: Schematic diagram on the kretchmann configuration.

© COPYRIGHT UPM

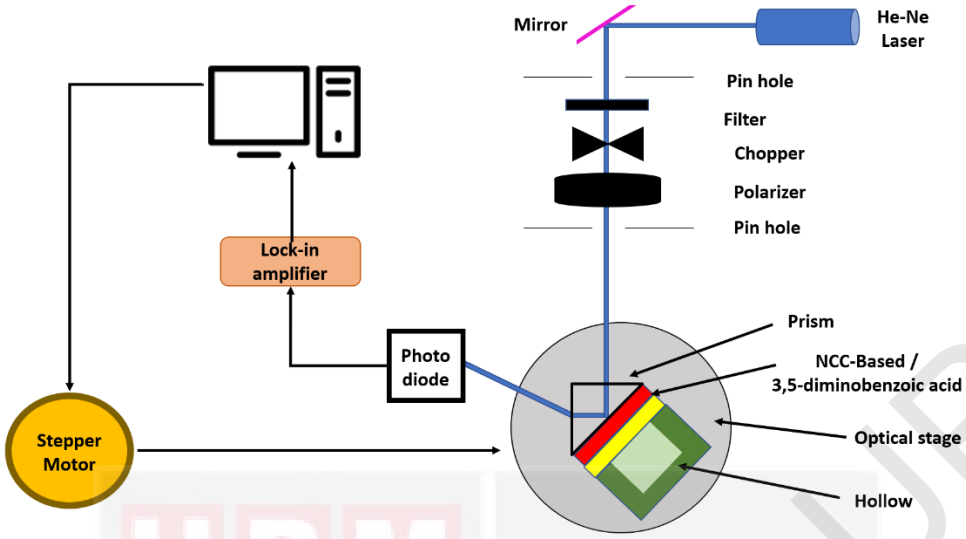

Figure 3.9: Experimental setup of SPR sensor.

3.2 Preparation of Active Layer

3.2.1 Preparation Chemicals

3,5-diaminobenzoic acid (DIABA) and Nanocellulose crystalline (NCC) with 98% purity were purchased from Sigma Aldrich. To prepare NCC solution, 5 g of NCC was diluted in 100 mL of deionized water. Then stir for 30 minutes. To prepare DIABA solution, 1.52 g of DIABA was diluted in 100 mL of deionized water. Then stir for 30 minutes. To prepare DIABA/NCC solution, DIABA solution was dropped into NCC solution drop by drop by ratio 2:1 while heat stir at 60 °C and left it for 24 hours. Then, the DIABA/NCC solution was proceed using centrifuge process for 15 minutes at 3000 rev/min.

3.2.2 Preparation of Thin Film

Distilled water or acetone has been used to clean the glass slips (24 mm × 24 mm × 0.1 mm) to remove any dust or fingerprint on the surface of the glass. Then, the glass slips were coated with gold layer by using SC7640 Sputter Coater (current setting = 20 mA) for

© COPYRIGHT UPM

67 sec to produce a 50 nm thickness of the gold layer to obtain an optimum dip in SPR curve. By the was set, the thickness of coated gold was determined. Then, about 0.5 mL DIABA diluted solution was added on the gold-coated glass and spun at 5000 rev/min for 30 seconds using spin coating system. Then, another glass slips have been used to prepare the gold thin film. 0.5 mL NCC diluted solution was added on the gold-coated glass and spun at 5000 rev/min for 30 seconds using the spin coating system. Lastly, the gold thin film was added by 0.5 mL DIABA/NCC solution and spun at 5000 rev/min for 30 seconds using spin coating system. Figure 3.10 shows the preparation process of the DIABA, NCC and DIABA/NCC based thin film graphically.

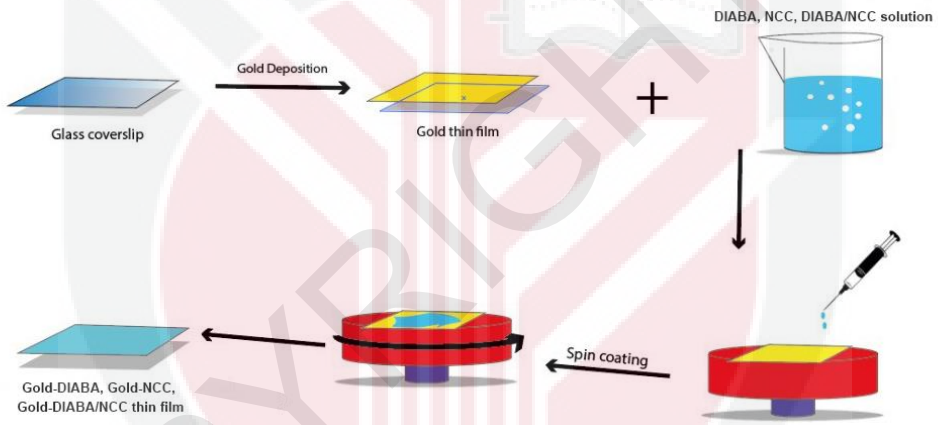

Figure 3.10: Preparation process of the DIABA, NCC and DIABA/NCC based thin films.

3.3 Preparation of Caffeine Solution

Caffeine powder ($C_8H_{10}N_4O_2$, M = 194.18 g/mol) was purchased from Sigma Aldrich. (caffeine). The caffeine was diluted by using formula $M_1V_1 = M_2V_2$ to prepare various concentration of solution. The caffeine with concentration 0.5 nM, 1 nM, 5 nM, 10 nM, 20 nM, 50 nM, 100 nM was produced by using the deionized water.

3.4 Surface Performance towards Caffeine

3.4.1 Surface Plasmon Resonance Reflectance

When a thin metal film hit by the plane-polarized light as shown in Figure 3.1.8 at an angle which equal to or greater than critical angle, the evanescent wave is created at the interface between prism and metal. When the vector of evanescent wave and surface plasmons have the same frequency, the excitation of surface plasmon resonance will occur. The transfer of energy from incoming light to surface plasmons occurs when surface plasmons are excited at the metal/dielectric interface which reducing the intensity of reflected light. Then, due to the efficient energy transferred to surface plasmons, a sharp dip was observed at an angle known as resonance angle, θ_{spr} as shown in Figure 3.11 (Gupta and Verma, 2009). The SPR sensor works by finding the change in the resonance angle ($\Delta\theta$).

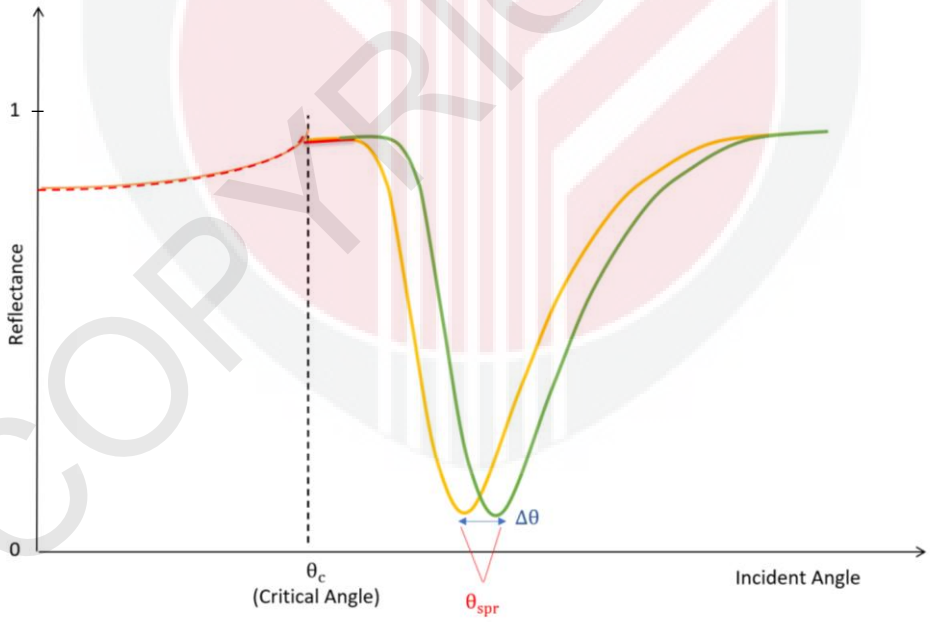

Figure 3.11: Graph of reflectance as a function of incident angle.

© COPYRIGHT UPM

3.4.2 Sensitivity

The sensitivity is computed by dividing changes in caffeine concentration by the slope of changes in resonance angle shift, ΔC which can be expressed as

$$S = \frac{\Delta\theta}{\Delta C} \tag{3.1}$$

the sensitivity of DIABA, NCC and DIABA/NCC thin films in sensing caffeine was obtained by plotting graph of resonance angle shift against concentration.

3.4.3 Binding affinity

Binding affinity is the strength of a biomolecule's binding interaction with its ligand or binding partner. The equilibrium dissociation constant (K_d), which is used to quantify and rank order the strengths of bimolecular interactions, is used to evaluate and report binding affinity. The lower the K_d value, the higher the ligand's binding affinity for its target. The weaker the attraction and binding between the target molecule and the ligand, the higher the K_d value.

The binding affinity between caffeine and sensing layer which are DIABA, NCC and DIABA/NCC can be obtained using Equation 3.2.

$$\Delta\theta = \frac{(\Delta\theta_{max} C)}{\frac{1}{K} + C} \tag{3.2}$$

where $\Delta\theta_{max}$ is the maximum SPR shift at the saturation, C is the caffeine concentration and K is the affinity constant.

3.4.4 Full Width Half Maximum

The angular width of the SPR curve at the half value of the maximum reflectance is described as full width at half maximum (FWHM). SPR curve can be calculated as the

© COPYRIGHT UPM

FWHM and the calculations were made for all concentrations of caffeine. It can be determined as the distance between the curve points at the peak half maximum level from the graph. A vertical line from the peak maximum to baseline was measured and it is divided by 2 to find the centre of the line. Figure 3.12 shows the example of determining FWHM.

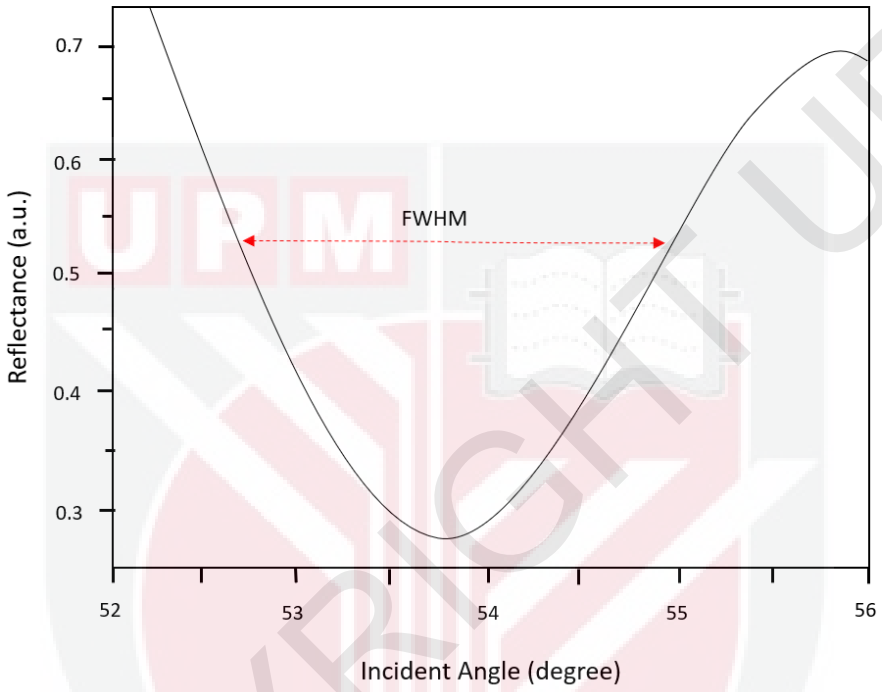

Figure 3.12: Example on determining FWHM.

© COPYRIGHT UPM

CHAPTER 4

RESULT AND DISCUSSION

4.1 Introduction

This chapter will review and discuss the results collected from the conducted experiments and also from sample prepared from the methodology in Chapter 3. This chapter divided into four parts for the detection of caffeine by SPR technique using four different sensing layers. The SPR sensor was started with the gold single layer and followed by gold-modified 3,5-diaminobenzoic acid (Gold-DIABA), gold-modified nanocellulose crystalline (Gold-NCC), and gold-modified combination of DIABA and NCC (Gold-DIABA/NCC). The analysis part contains the SPR signal, sensitivity, binding affinity, full width half maximum (FWHM), data accuracy (DA) and signal-to-noise-ratio (SNR). Its will be discussed one by one for each sensing layer.

4.2 SPR Analysis on Gold Thin Film

4.2.1 SPR Signal for Caffeine Solution

Firstly, a preliminary SPR test was conducted on gold sensing layer where deionized water was injected into the cell and in contact with the gold film. About 2 mL of deionized water was injected to ensure that it was contacted with the gold and the water level reaches the laser hit spot. The resonance angle obtained from the graph is 53.48° where this angle was used to compare the changes in resonance angle for different concentration of caffeine solution.

The SPR experiment was then carried out using different concentration of caffeine in aqueous solution. Starting from the lowest concentration (0.5 nM) until the highest (100 nM),

© COPYRIGHT UPM

each of the concentrations was injected one after another into the cell to make contact with the gold layer and the experiment was repeated two times in order to observe the accuracy of the data. The SPR curves of different concentration of caffeine solutions are shown in Figure 4.1. It is observed that there is no change in refractive index of the thin film and thus resulting resonance angle for all concentrations are same as shown in Table 4.1.

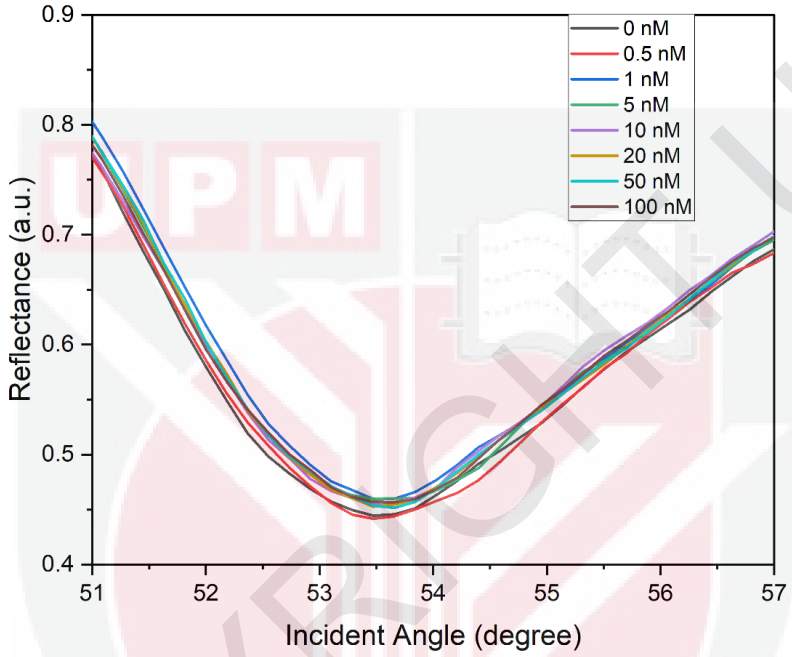

Figure 4.1: Reflectance curves for caffeine solution (0–100 nM) in contact with gold thin film (0 represent deionized water).

Table 4.1: Resonance angle and shift of resonance angle for caffeine solution (0-100 nM) using gold thin film.

Concentration of caffeine (nM)	Resonance angle, θ (degree)	Shift of resonance angle, $\Delta\theta$ (degree)
0	53.4801	0.0000
0.5	53.4801	0.0000
1	53.4801	0.0000
5	53.4801	0.0000
10	53.4801	0.0000
20	53.4801	0.0000

© COPYRIGHT UPM

50	53.4801	0.0000
100	53.4801	0.0000

4.2.2 Full Width Half Maximum and Detection Accuracy

Full width half maximum (FWHM) known as the angular width of the SPR curve for the half value of the maximum reflectance. Theoretically, Omar et al., (2019) reported the SPR curves should be as small as possible for FWHM in order to minimize the error in determining the reflectance. The width of the reflectivity curve corresponding to the half value of the maximum reflectance will be used to calculate FWHM. The FWHM of the SPR curve were calculated for all concentrations of caffeine detection with gold thin film and plotted as shown in Figure 4.2. The FWHM value decreased from 3.22° for deionized water to 3.20° and 3.19° for 0.5 nM and 1 nM. From the lowest, the value then increased to 3.22°, 3.23°, 3.31° and 3.31° for 5 nM, 10 nM, 20 nM and 50 nM caffeine solution, respectively. The highest value is at 3.31° for 50 nM concentration. It might be due to the intensified internal loss produced by the increase in total thickness of gold (Daniyal et al., 2018).

Detection accuracy (DA) depends on the width of SPR curve and it is inversely proportional to the FWHM. The higher FWHM SPR curve will produce lower DA. The DA of the SPR sensor for caffeine detection using gold thin film was shown in Figure 4.2. The 1 nM caffeine concentration records the highest DA for SPR sensor using gold thin film as the FWHM value is the lowest. The value of FWHM less than 1° is more likeable for better detection accuracy. However, this result showed value higher than 1° were probably because of the intensified loss produced by the increase in total thickness of gold (Daniyal et al., 2019).

© COPYRIGHT UPM

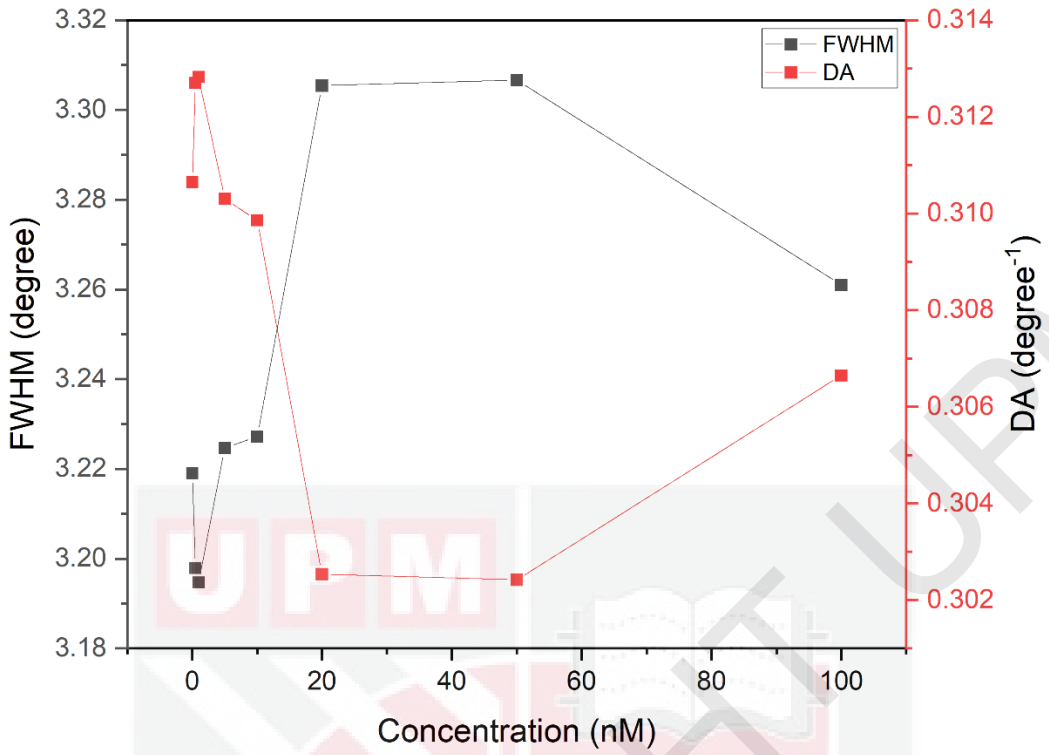

Figure 4.2: FWHM and DA for gold thin film in caffeine detection.

4.3 SPR Analysis on Gold-Modified 3,5-Diaminobenzoic Acid (Gold-DIABA) Thin Film

4.3.1 SPR Signal for Caffeine Solution

Firstly, SPR was performed with DIABA on the gold surface for deionized water. The resonance angle obtained was 53.47°. The SPR experiment was then conducted using different concentration of caffeine in aqueous solution from the lowest concentration (0.5 nM) until the highest (100 nM), each of the concentrations was injected one after another into the cell to attach with the sensing layer and the experiment was ran twice in order to observe the accuracy of the data. The reflectance curves of different concentration of caffeine solutions are shown in Figure 4.3. It can be concluded that there is no change in refractive index of the thin film and thus resulting resonance angle for all concentrations are same (Rosddi et al., 2021).

© COPYRIGHT UPM

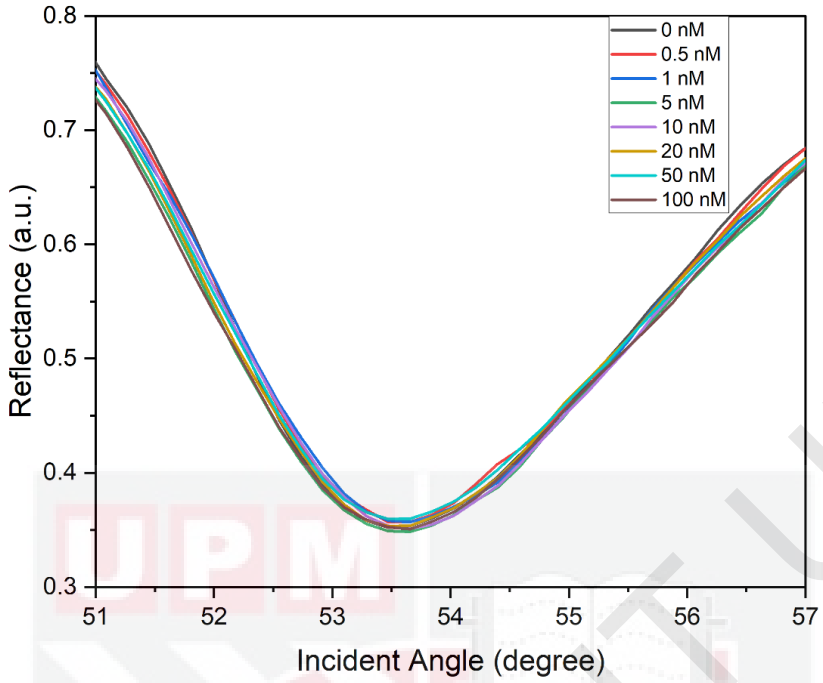

Figure 4.3: Reflectance curves for caffeine solution (0–100 nM) in contact with gold-modified DIABA thin film (0 represent deionized water).

Table 4.2: Resonance angle and shift of resonance angle for caffeine solution (0-100 nM) using gold-modified DIABA thin film.

Concentration of caffeine (nM)	Resonance angle, θ (degree)	Shift of resonance angle, $\Delta\theta$ (degree)
0	53.4719	0.0000
0.5	53.4719	0.0000
1	53.4719	0.0000
5	53.4719	0.0000
10	53.4719	0.0000
20	53.4719	0.0000
50	53.4719	0.0000
100	53.4719	0.0000

© COPYRIGHT UPM

4.2.2.4 Full Width Half Maximum and Detection Accuracy

The width of the reflectivity curve corresponding to the half value of the maximum reflectance was used to calculate for all concentrations of caffeine detection with gold-DIABA thin film and plotted as shown in Figure 4.4. The FWHM value went up dramatically from 2.88° for deionized water to 2.89°, 2.91°, 2.94° and 2.95° from 0.5 nM to 10 nM. Then, the value gradually increased to 2.95°, 2.97° and 2.98° for 20 nM, 50 nM and 100 nM. The peak value FWHM for the SPR curve caffeine detection using gold-DIABA was 2.98° for 100 nM.

The DA of the SPR sensor for caffeine detection using gold-DIABA thin film was shown in 4.4. The value 0.35/° for deionized water records the highest DA for SPR sensor using gold-DIABA thin film as the FWHM value is the lowest.

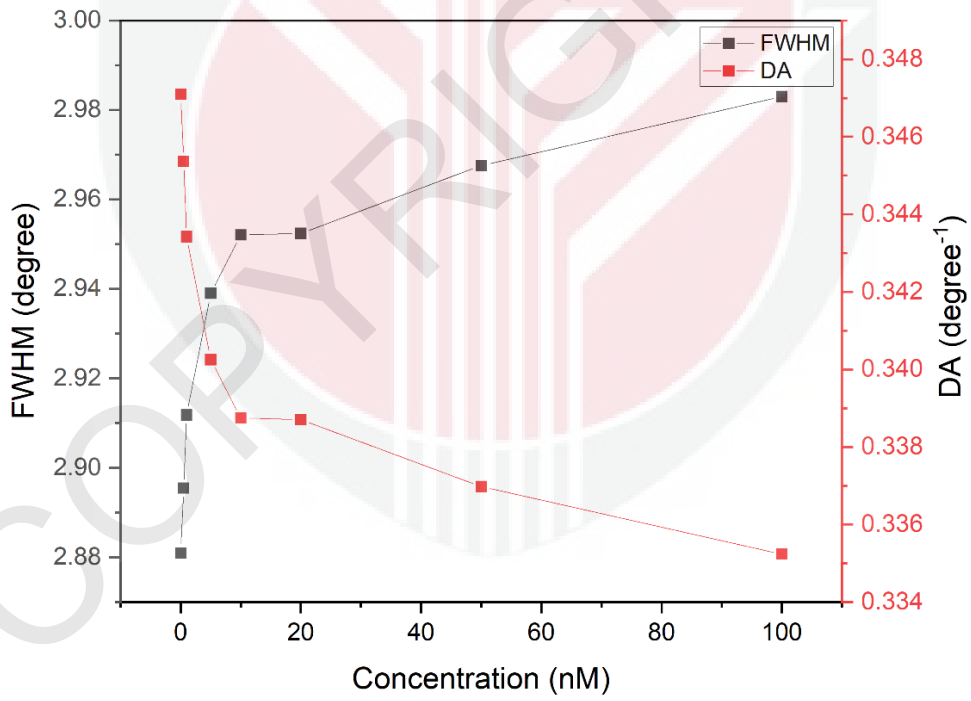

Figure 4.4: FWHM and DA for gold-modified DIABA thin film in caffeine detection.

© COPYRIGHT UPM

4.3 SPR Analysis on Gold-Modified Nanocellulose Crystalline (Gold-NCC) Thin Film

4.3.1 SPR Signal for Caffeine Solution

The SPR experiment was conducted on gold-NCC sensing thin film for deionized water with the same procedure. The resonance angle obtained from the graph is 54.22°. The resonance angle for caffeine detection using gold-NCC showed a positive shifted compared to caffeine detection using gold and gold-DIABA thin films. It means there was change in refractive index after the sensing layer contacted with the solution. The SPR experiment was then carried out using different concentration of caffeine in aqueous solution. Every concentration of caffeine solution was injected one by one into the cell and the data accuracy was observed by repeat the experiment twice. The reflectance curves of different concentration of caffeine solutions are shown in Figure 4.5. It is observed that there is also no change in resulting resonance angle for all concentrations are same due to the similar refractive index of the thin film.

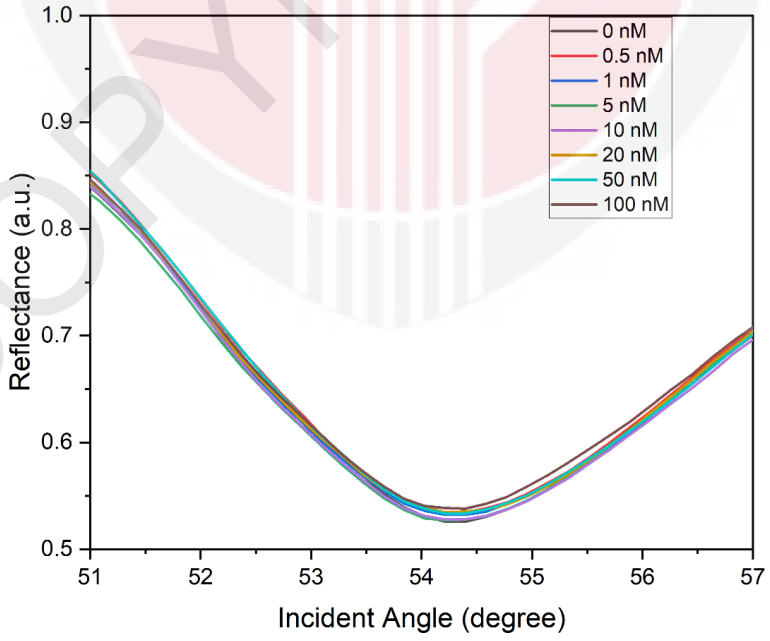

Figure 4.5: Reflectance curves for caffeine solution (0–100 nM) in contact with gold-modified NCC thin film (0 represent deionized water).

© COPYRIGHT UPM

Table 4.3: Resonance angle and shift of resonance angle for caffeine solution (0-100 nM).

Concentration of caffeine (nM)	Resonance angle, θ (degree)	Shift of resonance angle, $\Delta\theta$ (degree)
0	54.2241	0.0000
0.5	54.2241	0.0000
1	54.2241	0.0000
5	54.2241	0.0000
10	54.2241	0.0000
20	54.2241	0.0000
50	54.2241	0.0000
100	54.2241	0.0000

4.3.2 Full Width Half Maximum and Detection Accuracy

Using the same procedure as earlier, FWHM value for all concentration were obtained and plotted as shown in Figure 4.6. The FWHM value rise drastically from 3.30° for deionized water to 3.37° and 3.44° for 0.5 nM and 1 nM caffeine solution. Then, the value slightly increased for 5 nM and gradually increased to 3.46° for 10 nM. Then, it went up to the peak at 3.47° for 20nM. For concentration 50 nM, the FWHM then suddenly drop to 3.44° and slightly increased again to 3.45° for 100 nM. The highest FWHM value is 3.47° for 20 nM concentration might be due to the intensified internal loss due to the increase in total thickness of sensor (Hashim et al., 2020).

DA depends on the width of SPR curve and it is inversely proportional to the FWHM. The lower FWHM value will produce higher DA. The DA of the SPR sensor for caffeine detection using gold-NCC thin film was shown in 4.6. The value 0.30/° for deionized water records the highest DA for SPR sensor using gold-NCC thin film.

© COPYRIGHT UPM

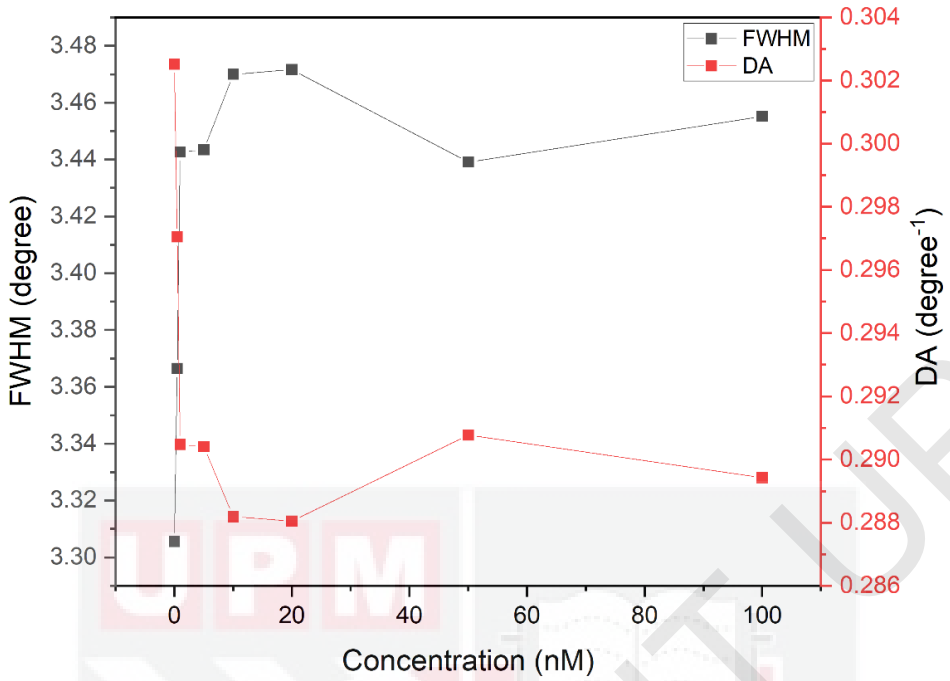

Figure 4.6: FWHM and DA for gold-modified NCC thin film in caffeine detection.

4.4 SPR Analysis on Gold-Modified DIABA/NCC (Gold-DIABA/NCC) Thin Film

4.4.1 SPR Signal for Caffeine Solution

Then, the SPR experiment was repeated with the same procedure on gold-DIABA/NCC for deionized. The resonance angle obtained from the graph was 54.79°. The SPR curve for deionized water using gold-DIABA/NCC showed bigger positive shift compared to SPR curve using gold, gold-DIABA and gold-NCC thin films. The SPR experiment was then carried out starting from the lowest until the highest caffeine concentrations by injecting each of them into the cell in a time. The SPR curves of different concentration of caffeine solutions are shown in Figure 4.7. It is observed that there were changes in refractive index of the thin film and thus resulting resonance angle for all concentrations are different. The resonance angle was measured decreased to 54.69°, 54.63°, 54.47°, 54.45°, 54.43°, 54.41° and 54.39° respectively for 0.5 nM until 100 nM concentrations of caffeine solution, respectively. The negative shift

© COPYRIGHT UPM

for SPR curve behaviour might be due to various reasons such as the reduction of the thickness of the sensing layer (Saha and Sarkar, 2016).

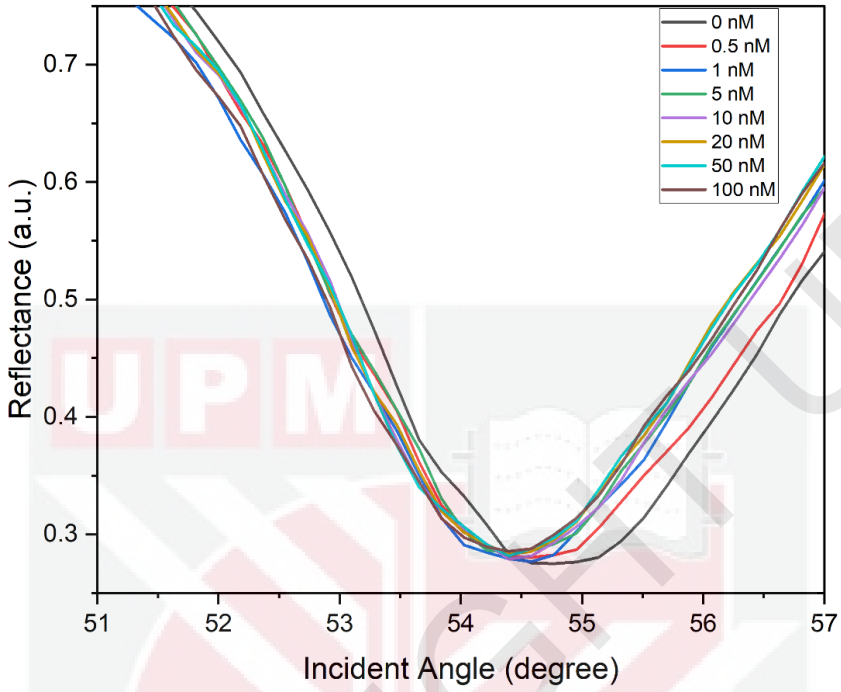

Figure 4.7: Reflectance curves for caffeine solution (0–100 nM) in contact with gold-modified DIABA/NCC thin film (0 represent deionized water).

Table 4.4: Resonance angle and shift of resonance angle for caffeine solution (0-100 nM) using gold-modified DIABA/NCC thin film.

Concentration of caffeine (nM)	Resonance angle, θ (degree)	Shift of resonance angle, $\Delta\theta$ (degree)
0	54.7873	0.0000
0.5	54.6944	0.0929
1	54.635	0.1523
5	54.4665	0.3208
10	54.4519	0.3354
20	54.4385	0.3488
50	54.4135	0.3738
100	54.3885	0.3988

© COPYRIGHT UPM

4.4.2 Sensitivity

The shift of resonance angle ($\Delta\theta$) was introduced as a parameter to measure the sensor sensitivity (Ramdzan et al., 2019). The resonance angle and shift of resonance angle for different concentrations of caffeine contact with gold-DIABA/NCC thin film was shown in Figure 4.8. The sensitivity of sensing layer with different concentrations of caffeine solutions was also determined by plotting the graph between the concentrations and the shift of resonance angle, $\Delta\theta$. Based on the linear regression graph, the plotted data was separated into 2 regions; deionized water to 5 nM and 10 nM to 100 nM concentrations caffeine solution.

The value of linear regression coefficient R^2 for first region was 0.90946 and the relationship between the SPR angle shift and caffeine concentrations was governed by Eq. ($\Delta\theta_{SPR}$) = 0.05629[Caffeine] + 0.05003. Whereas, the value of R^2 for the second region is 0.96867 and ($\Delta\theta_{SPR}$) = 6.8245×10^{-4}[Caffeine] + 0.3335. The gradient of the plotted graph is defined as the sensitivity of sensing layer toward caffeine detection. The first region's linear regression analysis yielded a gradient of 0.05629° nM^{-1}, whereas the second region's yielded a gradient of 6.8245×10^{-4} nM^{-1}. It displayed more sensitivity for lower concentration compared to the higher concentration of the caffeine solution. Therefore, it can be concluded that gold-DIABA/NCC layer was sensitive towards caffeine and show a good sensor sensitivity for SPR performance in caffeine detection.

© COPYRIGHT UPM

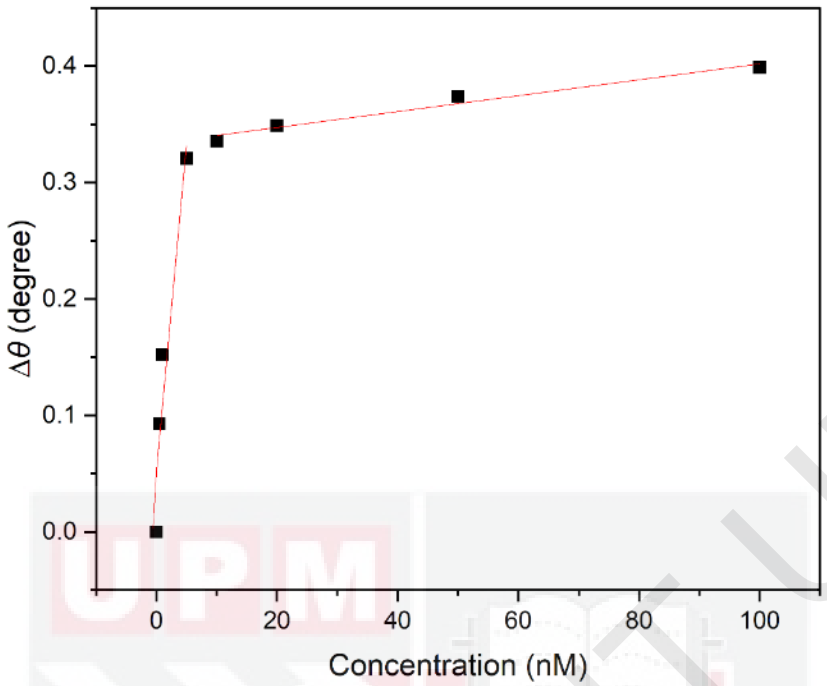

Figure 4.8: Resonance angle shift of gold-modified DIABA/NCC surface in contact with different caffeine concentrations.

4.4.3 Binding Affinity

The value of binding affinity constant, *K* was also derived by plotting the saturation values for the shift of resonance angle, $\Delta\theta$ with the increasing of caffeine concentration. By fitting the data from Table 4.4 using Langmuir isotherm model, the binding affinity of the caffeine towards the gold-DIABA/NCC sensing layer can be obtained using Langmuir equation which is

$$\Delta\theta = \frac{\Delta\theta_{max} C}{\frac{1}{K} + C} \tag{3.2}$$

From the equation, $\Delta\theta_{max}$ is the maximum SPR angle shift at the saturation, *C* is the concentration of the caffeine solution and *K* is the binding affinity constant. The plots which were fitted using Origin Pro fitting tool in the Langmuir model is shown in Figure 4.9. The

© COPYRIGHT UPM

fitting yielded an R^2 value of 0.994°. From the graph, the value of K was determined to be also 0.6655 M^{-1}.

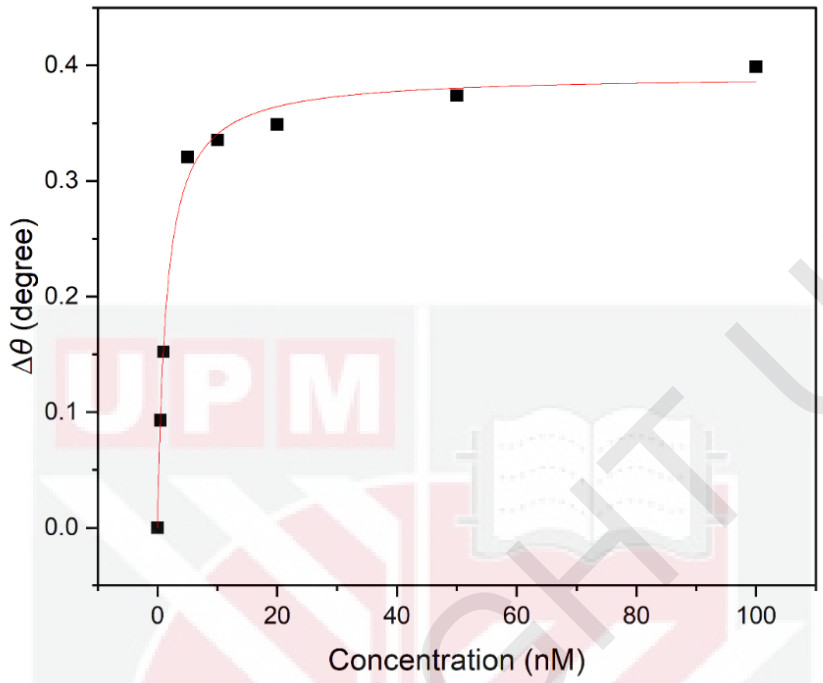

Figure 4.9 Langmuir isotherm model caffeine in contact with gold-modified DIABA/NCC thin film.

4.4.4 Full Width Half Maximum and Detection Accuracy

The FWHM and DA value was measured using the same method for all caffeine concentrations. Both data plotted in a graph as shown in Figure 4.10. The FWHM value rise drastically from 2.96° for deionized water to 2.99° and 3.04° for 0.5 nM and 1 nM caffeine solution. Then, the value slightly increased for 5 nM and 10 nM to 3.05° and 3.06°. Then, it went down to 3.04° for 20 nM gradually decreased to 3.02° for 50 nM. Then, the value rises up drastically to 3.21° for 100 nM. The highest FWHM value is 3.21° for 100 nM concentration might be due to the intensified internal loss due to the increase in total thickness of sensor (Hashim et al., 2020). The FWHM values are lower from 20 to 50 nM compared 5 nM and 10

© COPYRIGHT UPM

nM concentration may be caused by the functional groups in modified DIABA/NCC layer which will reduced the scattering of free electrons (Zijlstra et al., 2012).

The DA of the SPR sensor for caffeine detection using gold-DIABA/NCC thin film is shown in 4.10. The value 0.34/° for deionized water records the highest DA for SPR sensor using gold-DIABA/NCC thin film as the FWHM value is the lowest.

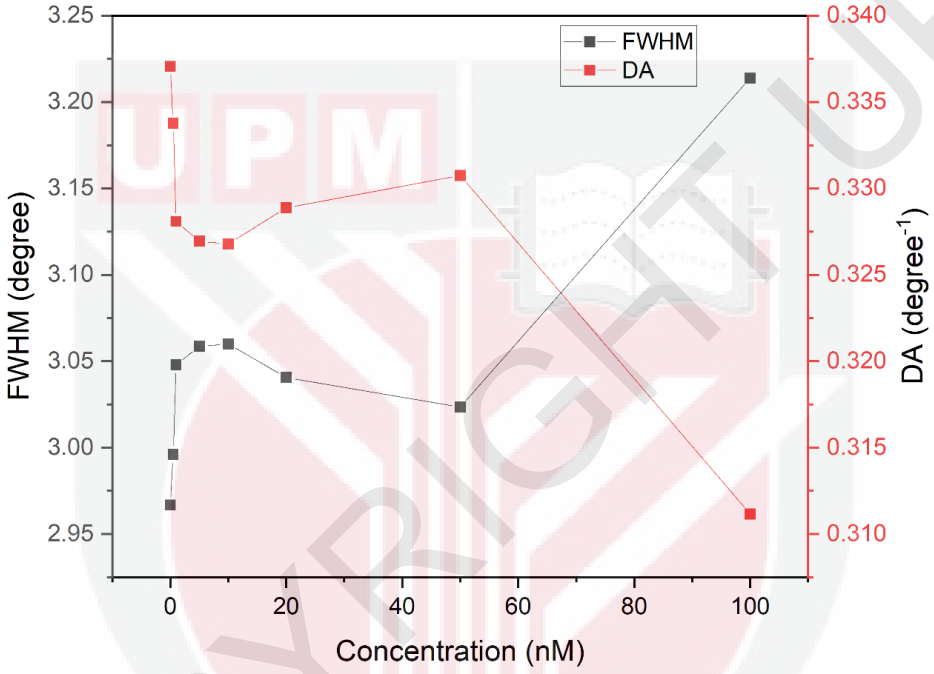

Figure 4.10: FWHM and DA for gold-modified DIABA/NCC thin film in caffeine detection.

4.4.5 Signal-to-Noise Ratio

The signal-to-noise ratio (SNR) can be defined as the basic figure-of-merit (FOM) of SPR. It can be obtained from SPR sensor apart from the sensitivity. It also one of the important parameters and was calculated by multiplying the DA value with the shift of resonance angle, $\Delta\theta$. Figure 4.20 shows the SNR of the sensor for caffeine using gold-modified DIABA/NCC thin film. As the caffeine concentration increases, the SNR of the SPR sensor is also increases. As refer to Figure 4.11, it can be observed that the SNR plotted is almost similar to the plotting

© COPYRIGHT UPM

for sensitivity. This proved that resonance shift angle, $\Delta\theta$ has bigger effect in determining the SNR value compared to the DA (Kamaruddin et al. in 2016).

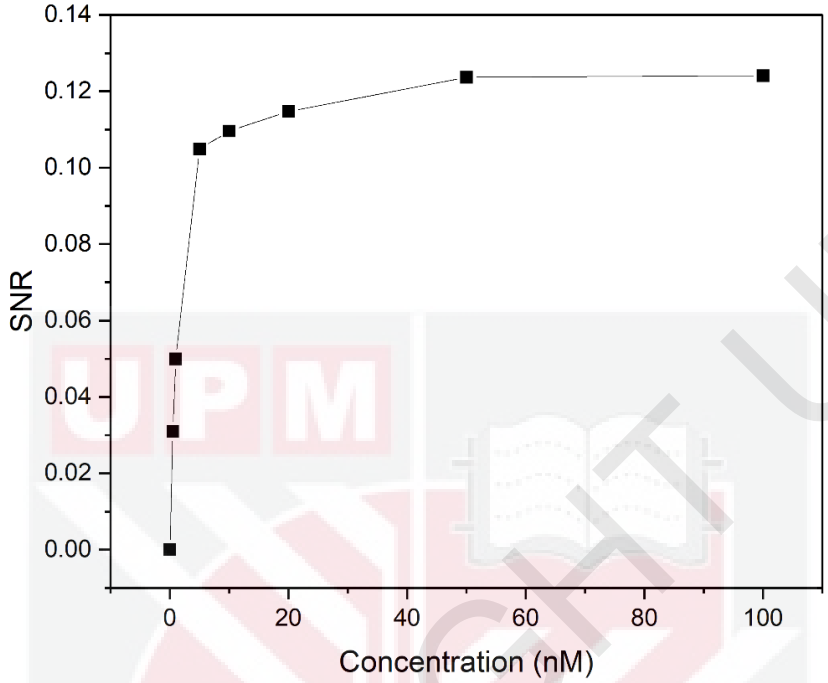

Figure 4.11: SNR for gold-modified DIABA/NCC thin film in caffeine detection.

4.5 Comparison for Gold, Gold-DIABA, Gold-NCC and Gold-DIABA/NCC Thin Films

4.5.1 SPR Signal for Deionized Water

Lastly, the SPR curve results for all different sensing layer were compared to each other. The data for caffeine detection of deionized water using gold, gold-DIABA, gold-NCC and gold-DIABA/NCC were transferred to a new datasheet. By using Origin Pro, a graph for SPR curve between reflectance and incident angle was plotted as shown in Figure 4.12. From data reported in previous part, the SPR resonance angle for deionized water using gold, gold-DIABA, gold-NCC and gold-DIABA/NCC was 53.48°, 53.47°, 54.22° and 54.79°, respectively. It showed that the value of resonance angle for sensing deionized water using

© COPYRIGHT UPM

modified thin films increases compared to single gold layer thin film except for DIABA. The layer might be eroded due to DIABA was on of hydrophilic monomer (Mehrparvar and Rahimpour, 2015). Moreover, the SPR curve obtained using gold-NCC and gold-DIABA/NCC thin film shifted to the right as shown in Figure 4.21. It also can be observed that gold-DIABA/NCC thin film has higher shift compared to gold-NCC thin film. The sensing layer gold-DIABA/NCC showed a biggest of SPR curve shifted to the right. It might be due to the change in refractive index of the thin film when deionized water makes contact with thin films (Gupta and Verma, 2009).

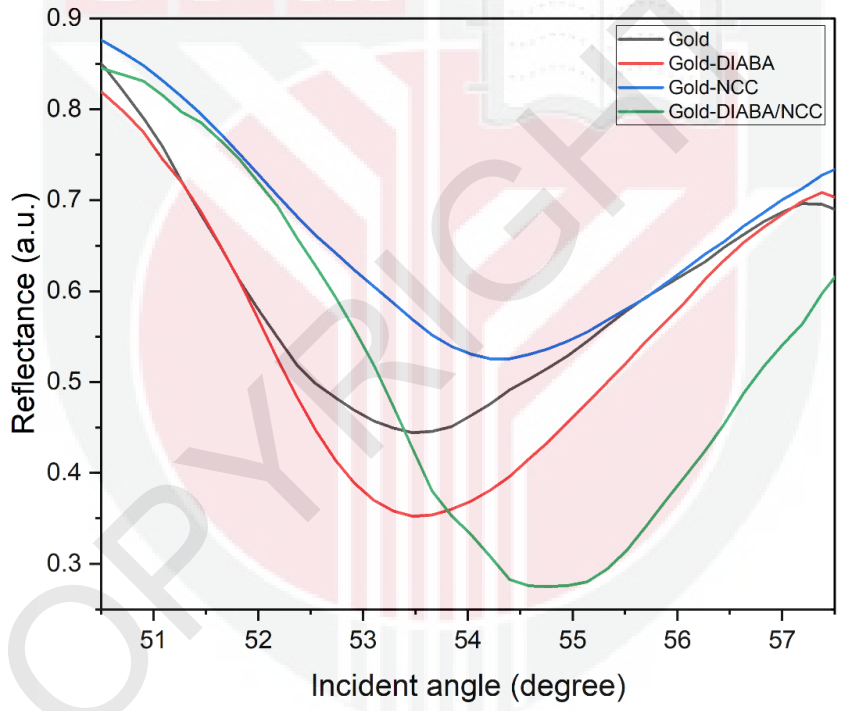

Figure 4.12: Reflectance curves for deionized water in contact with all different sensing thin films.

© COPYRIGHT UPM

4.5.2 Sensitivity

The shift of resonance angle for different concentrations of caffeine contact with gold, gold-DIABA, gold-NCC and gold-DIABA/NCC are shown in Table 4.5. The sensitivity of all sensing layers was determined by plotting the graph between caffeine concentrations and the shift of resonance angle, $\Delta\theta$. Based on the linear regression graph in Figure 4.13, the resonance angle for caffeine concentrations shows no change when it is in contact with gold, gold-DIABA and gold-NCC. The value of linear regression coefficient R^2 for all of them was 0 and the relationship between the SPR angle shift and caffeine concentrations was ($\Delta\theta_{SPR}$) = 0[Caffeine] + 0. The gradient of the plotted graph is defined as the sensitivity of sensing layer toward caffeine detection. Therefore, it can be concluded that gold, gold-DIABA and gold-NCC are not sensitive towards caffeine.

Also based on Figure 4.13, the contact between caffeine concentrations and gold-DIABA/NCC showed change in resonance angle. Its gradient value of first and second region's linear regression analysis obtained higher compared to other thin films which are 0.05003 nM^{-1} and 6.8245×10^{-4} nM^{-1}. It might be caused by the optimum thickness of the sensing layer was obtained by this thin (Vahed and Nadri, 2019). The value of linier regression coefficient R^2 also higher which are 0.90946 and 0.96867 for both regions as stated in section 4.2.4.2. Therefore, it can be concluded that gold-DIABA/NCC layer was more sensitive towards caffeine than other sensing layers.

© COPYRIGHT UPM

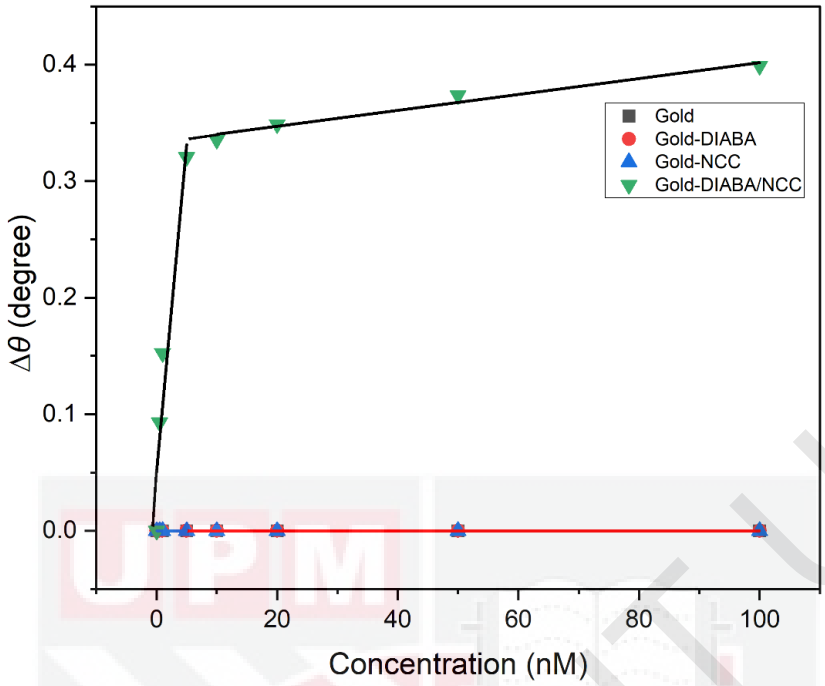

Figure 4.13 Resonance angle shift of caffeine concentrations in contact with different thin films.

4.5.3 Binding Affinity

The binding affinity for all thins films was compared. It is essential to determine the affinity between the analyte and immobilised ligands of an SPR sensor. It also used to ensure the strength and evanescent field stabilization in order to detect whole range caffeine concentrations (Kamaruddin et al. 2017). The binding affinity of caffeine solution towards all thin films were fitted using Origin Pro fitting tool in the Langmuir model are shown in Figure 4.14.

From Equation 3.2, $\Delta\theta_{max}$ is the maximum SPR angle shift at the saturation, C is the concentration of the caffeine solutions and K is the binding affinity constant. From the graph, the value of K was determined to be 0.6655 M^{-1} and the fitting yielded an R^2 value of 0.994° for gold-DIABA/NCC thin film. Furthermore, the other sensing layer show no value for R^2 and 0.9946 for value of K. In conclusion, the greater affinity of caffeine for the modified gold

© COPYRIGHT UPM

thin film demonstrated that the DIABA/NCC material helps to improve the SPR optical sensor's sensitivity (Daniyal et al. 2019).

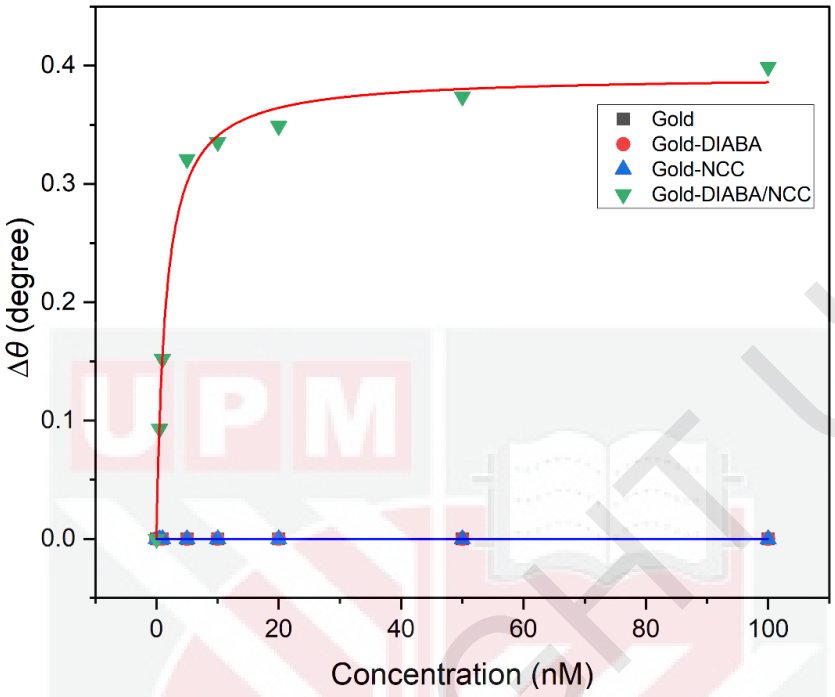

Figure 4.14: Langmuir isotherm model caffeine in contact with thin films.

4.5.4 Full Width Half Maximum and Detection Accuracy

Next, the procedure was repeated to calculate the FWHM and DA values. FWHM and DA value for each sensing layer transferred into a datasheet as shown in Table 4.5. The FWHM data was plotted in the same graph to be compared. From Figure 4.15, the highest value of FWHM was obtained gold-modified NCC with the highest value at 3.47° at 20 nM caffeine concentrations. Then, the value of FWHM for gold thin film for 20 nM most similar to FWHM value for gold-modified NCC for deionized water. Next, FWHM value for gold-modified NCC/DIABA initially showed far more below than the gold thin film graph. Besides, at the end of the graph was quite closed to each other for 100 nM caffeine concentration. Next, FWHM for gold-modified DIABA shown at the bottom compared to others and the lowest

© COPYRIGHT UPM

point is at 2.88° for deionized water. Lastly, the trend for all graph seems similar to each other with begin from below and end at the higher point.

The DA value also collected in a datasheet to be compared and plotted as shown in Figure 4.16. As stated, that DA value will be inverse to the FWHM value. Overall, the highest DA value recorded was 0.35/° for SPR sensor using gold-modified DIABA thin film. Then, the lowest DA value was at 2.88/° for 20 nM records for SPR sensor using gold-modified NCC.

Table 4.5: FWHM and DA for caffeine solution (0-100 nM).

	FWHM (degree)				**DA ($\mathbf{degree^{-1}}$)**			
Conc-entration (nM)	**Gold**	**DIABA**	**NCC**	**DIABA /NCC**	**Gold**	**DIABA**	**NCC**	**DIABA /NCC**
0	3.219	2.881	3.306	2.967	0.311	0.347	0.303	0.337
0.5	3.198	2.895	3.366	2.996	0.313	0.345	0.297	0.334
1	3.195	2.911	3.442	3.048	0.313	0.343	0.290	0.328
5	3.225	2.939	3.443	3.059	0.310	0.340	0.290	0.327
10	3.227	2.952	3.469	3.060	0.309	0.339	0.288	0.327
20	3.305	2.952	3.472	3.041	0.303	0.339	0.288	0.329
50	3.307	2.968	3.439	3.023	0.302	0.337	0.291	0.331
100	3.261	2.983	3.455	3.214	0.307	0.335	0.289	0.311

© COPYRIGHT UPM

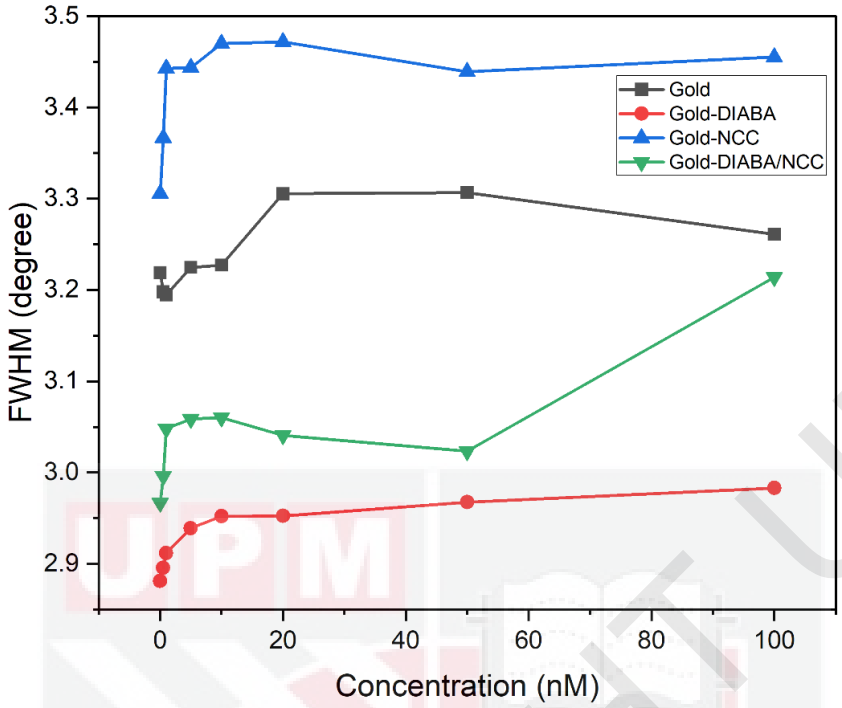

Figure 4.15: FWHM for different thin films in caffeine detection.

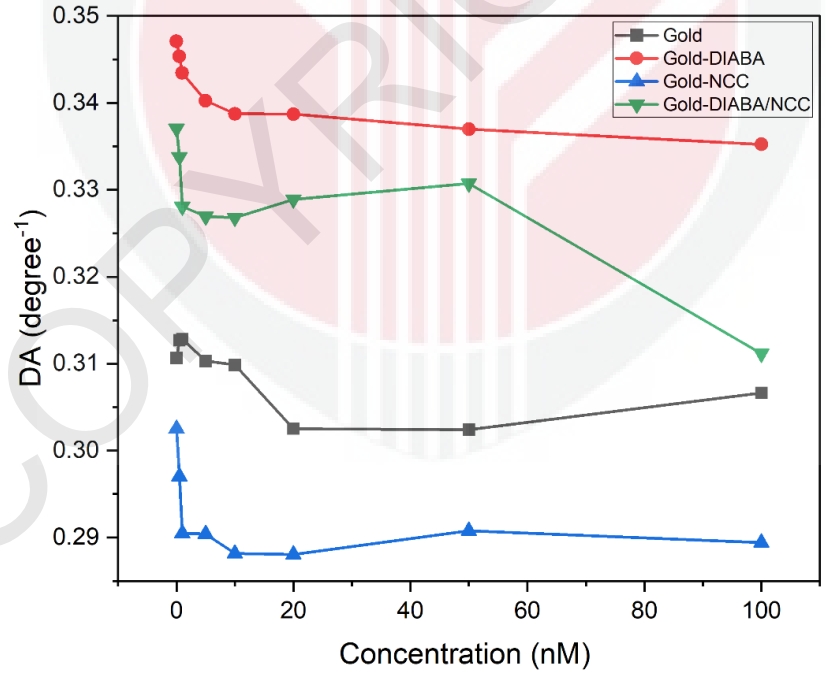

Figure 4.16: DA for different thin films in caffeine detection.

© COPYRIGHT UPM

4.2.5.5 Signal-to-Noise Ratio

The SNR is one of important parameters that can be calculated by multiplying the resonance angle shift, $\Delta\theta$ and DA value. It can be regarded as the basic figure-of-merit (FOM) of SPR. It can be obtained from SPR sensor apart from the sensitivity. Figure 4.17 shows the SNR of the sensor for caffeine using four different thin films. The value of SNR shows no change as the caffeine concentration increases by using gold, gold-modified DIABA and gold-modified NCC thin films. However, caffeine detection using gold-modified DIABA/NCC shows the value of SNR increases as the caffeine concentration increases. It can also be observed that the SNR plotted is almost similar to the plotting for gold-modified DIABA/NCC's sensitivity in Figure 4.17. This proved that resonance shift angle, $\Delta\theta$ has bigger effect in determining the SNR value compared to the DA as reported by Kamaruddin et al. (2016).

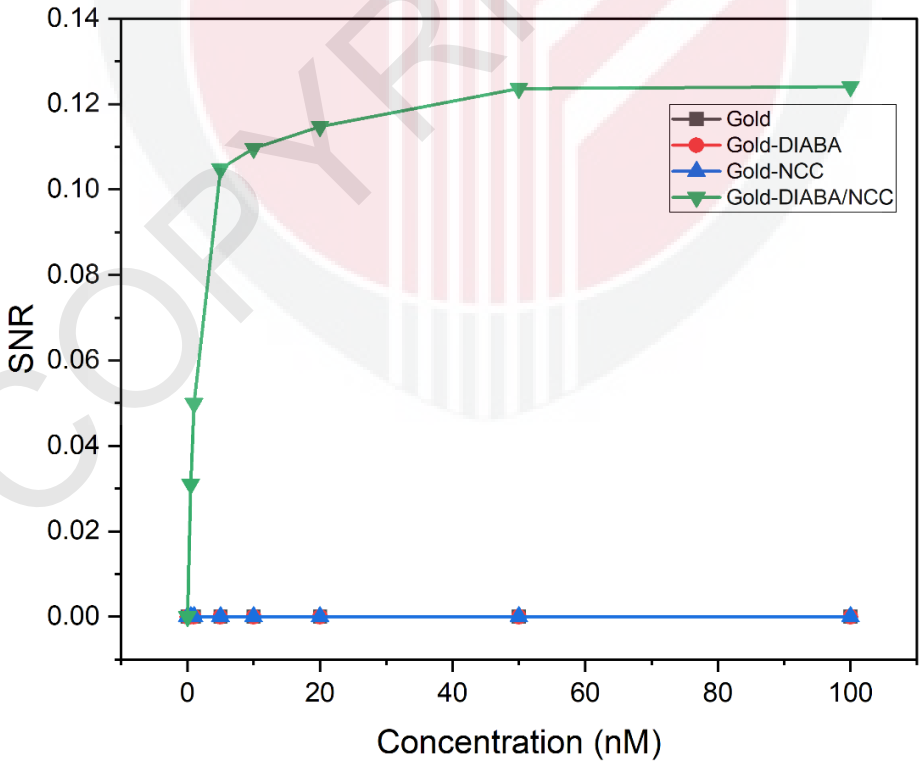

Figure 4.17: SNR for different thin films in caffeine detection.

© COPYRIGHT UPM

CHAPTER 5

CONCLUSION

5.1 Conclusion

The objective of this study was to study the detection of caffeine and to identify the improvement of sensitivity in caffeine detection by using DIABA and NCC using surface plasmon resonance technique. The study showed determination of different caffeine concentration ranging from 0.5-100 nM by four different thin films using surface plasmon resonance method. It reports that gold single layer and thin film coated by DIABA and NCC separately not sensitive enough towards caffeine solution. It shows no value for sensitivity because of no change resonance angle for different caffeine concentrations. It has been identified that gold thin film coated with DIABA/NCC was the most suitable thin film to be used for the SPR experiment. The sensitivity gained was of 0.05629° nM^{-1} and 6.8245×10^{-4} nM^{-1} for both regions. The binding affinity constant was 0.6655 M^{-1} and the lowest detection limit of caffeine solution reported was as low as 0.5 nM. The FWHM value calculated was 2.96°, 2.99°, 3.04°, 3.05°, 3.06°, 3.04°, 3.02° and 3.21°. It can be observed the highest detection accuracy (DA) is 0.34/° at 0 nM and the lowest is 0.31/° at 100 nM.

In conclusion, this study obtained that gold thin film coated with DIABA/NCC has a great potential in caffeine detection using SPR method. The study approach might make a significant contribution to society, primarily in the field of environmental sensing, and could be used in a wide range of optical-based applications.

5.1 Recommendation for Future Work

For future improvement, it would be interesting to study the interaction between these thin films and caffeine solutions to obtain significant knowledge for the characterisation using

© COPYRIGHT UPM

analysis method such as FTIR and FESEM. It might help in improvise the methodology in order to obtain the good results. Other than that, future study should obtain the impact of detecting the lower concentration of caffeine solutions. Last but not least, to improve the sensitivity and selectivity of the sensor for future study should be investigated with other material such as silver nitrate.

© COPYRIGHT UPM

REFFERENCES

Ahmad Bhawani, S., Fong, S. S., & Mohamad Ibrahim, M. N. (2015). Spectrophotometric analysis of caffeine. *International Journal of Analytical Chemistry*. https://doi.org/10.1155/2015/170239

Amin, A. S., & El-Henawee, M. M. (1995). Colorimetric method for the simultaneous determination of chlorphenoxamine hydrochloride and anhydrous caffeine in pure and dosage forms with rose bengal. *Mikrochimica Acta*, *118*(3–4), 177–183. https://doi.org/10.1007/BF01244357

Amos-Tautua, Bamidele Martin, W., & Diepreye, E. R. E. (2014). Ultra-violet spectrophotometric determination of caffeine in soft and energy drinks available in Yenagoa, Nigeria. *Advance Journal of Food Science and Technology*, *6*(2), 155–158. https://doi.org/10.19026/ajfst.6.2

Chen, X., Liu, Y., Jaenicke, E. C., & Rabinowitz, A. N. (2019). New concerns on caffeine consumption and the impact of potential regulations: The case of energy drinks. *Food Policy*, *87*, 101746. https://doi.org/10.1016/j.foodpol.2019.101746

Daniyal, W. M. E. M. M., Fen, Y. W., Abdullah, J., Sadrolhosseini, A. R., Saleviter, S., & Omar, N. A. S. (2018). Exploration of surface plasmon resonance for sensing copper ion based on nanocrystalline cellulose-modified thin film. *Optics Express*, *26*(26), 34880. https://doi.org/10.1364/oe.26.034880

Daniyal, W. M. E. M. M., Fen, Y. W., Abdullah, J., Sadrolhosseini, A. R., Saleviter, S., & Omar, N. A. S. (2019). Label-free optical spectroscopy for characterizing binding properties of highly sensitive nanocrystalline cellulose-graphene oxide based nanocomposite towards nickel ion. *Spectrochimica Acta - Part A: Molecular and Biomolecular Spectroscopy*, *212*, 25–31. https://doi.org/10.1016/j.saa.2018.12.031

© COPYRIGHT UPM

Daniyal, W. M. E. M. M., Fen, Y. W., Anas, N. A. A., Omar, N. A. S., Ramdzan, N. S. M., Nakajima, H., & Mahdi, M. A. (2019). Enhancing the sensitivity of a surface plasmon resonance-based optical sensor for zinc ion detection by the modification of a gold thin film. *RSC Advances*, *9*(71), 41729–41736. https://doi.org/10.1039/c9ra07368j

de Souza, M. L., Otero, J. C., & López-Tocón, I. (2020). Comparative performance of citrate, borohydride, hydroxylamine and β-cyclodextrin silver sols for detecting ibuprofen and caffeine pollutants by means of surface-enhanced raman spectroscopy. *Nanomaterials*, *10*(12), 1–14. https://doi.org/10.3390/nano10122339

Deng, H., Wang, B., Wu, M., Deng, B., Xie, L., & Guo, Y. (2019). Rapidly colorimetric detection of caffeine in beverages by silver nanoparticle sensors coupled with magnetic molecularly imprinted polymeric microspheres. *International Journal of Food Science and Technology*, *54*(1), 202–211. https://doi.org/10.1111/ijfs.13924

dePaula, J., & Farah, A. (2019). Caffeine consumption through coffee: Content in the beverage, metabolism, health benefits and risks. *Beverages*, *5*(2), 37. https://doi.org/10.3390/beverages5020037

Du, C., Ma, C., Gu, J., Li, L., & Chen, G. (2020). Fluorescence sensing of caffeine in tea beverages with 3,5-diaminobenzoic acid. *Sensors (Switzerland)*, *20*(3), 1–9. https://doi.org/10.3390/s20030819

Effects, P. H. (2012). *www.mpi.govt.nz*. *November*.

Fen, Y. W., & Yunus, W. M. M. (2013). Surface plasmon resonance spectroscopy as an alternative for sensing heavy metal ions: A review. *Sensor Review*, *33*(4), 305–314. https://doi.org/10.1108/SR-01-2012-604

Fen, Y. W., Yunus, W. M. M., & Yusof, N. A. (2012). Surface plasmon resonance optical

© COPYRIGHT UPM

sensor for detection of Pb 2+ based on immobilized p-tert-butylcalix[4]arene-tetrakis in chitosan thin film as an active layer. *Sensors and Actuators, B: Chemical*, *171–172*, 287–293. https://doi.org/10.1016/j.snb.2012.03.070

Ferreyra, C. F., & Ortiz, C. S. (2002). Simultaneous spectrophotometric determination of phenilpropanolamine HCL, caffeine and diazepam in tablets. *Journal of Pharmaceutical and Biomedical Analysis*, *29*(5), 811–818. https://doi.org/10.1016/S0731-7085(02)00130-9

Franzen, L., Anderski, J., & Windbergs, M. (2015). Quantitative detection of caffeine in human skin by confocal Raman spectroscopy - A systematic in vitro validation study. *European Journal of Pharmaceutics and Biopharmaceutics*, *95*, 110–116. https://doi.org/10.1016/j.ejpb.2015.03.026

Gamonchuang, J., & Burakham, R. (2021). Amino-based magneto-polymeric-modified mixed iron hydroxides for magnetic solid phase extraction of phenol residues in environmental samples. *Journal of Chromatography A*, *1643*, 462071. https://doi.org/10.1016/j.chroma.2021.462071

George, N. A., Thomas, N. B., Moidu, H. H., & Piyush, K. (2015). Optimization of an optical chopper-laser beam arrangement in low-frequency applications. *Optik*, *126*(23), 3628–3630. https://doi.org/10.1016/j.ijleo.2015.08.241

Ghosh, A. K., Ghosh, C., & Gupta, A. (2013). A simple approach to detect caffeine in tea beverages. *Journal of Agricultural and Food Chemistry*, *61*(16), 3814–3820. https://doi.org/10.1021/jf400293u

Gliszczyńska-Świgło, A., & Rybicka, I. (2015). Simultaneous determination of caffeine and water-soluble vitamins in energy drinks by HPLC with photodiode array and fluorescence detection. *Food Analytical Methods*, *8*(1), 139–146. https://doi.org/10.1007/s12161-014-

© COPYRIGHT UPM

9880-0

Goldbarg. (1953). The colorimetric determination of leucine aminopeptidase in urine and serum of normal. *Scientific Edition*, 283–291.

Gong, W., Zhang, L., Yu, Y., Lin, B., Wang, Y., Guo, M., & Cao, Y. (2021). A novel fluorescent strategy based on double modifications of metal organic framework material CAU-10-NH_2 for low background and high sensitivity determination of H_2S. *Talanta*, *229*, 122271. https://doi.org/10.1016/j.talanta.2021.122271

González, N., Lantmann Corral, S. P., Zanini, G., Montejano, H., & Acebal, C. C. (2020). An inner filter effect based sensing system for the determination of caffeine in beverage samples. *Analyst*, *145*(6), 2279–2285. https://doi.org/10.1039/c9an02483b

Gupta, B. D., & Verma, R. K. (2009). Surface plasmon resonance-based fiber optic sensors: Principle, probe designs, and some applications. *Journal of Sensors*. https://doi.org/10.1155/2009/979761

Hashim, H. S., Fen, Y. W., Sheh Omar, N. A., Abdullah, J., Daniyal, W. M. E. M. M., & Saleviter, S. (2020). Detection of phenol by incorporation of gold modified-enzyme based graphene oxide thin film with surface plasmon resonance technique. *Optics Express*, *28*(7), 9738. https://doi.org/10.1364/oe.387027

Homola, J., Yee, S. S., & Gauglitz, G. (1999). Surface plasmon resonance sensors: review. *Sensors and Actuators, B: Chemical*, *54*(1), 3–15. https://doi.org/10.1016/S0925-4005(98)00321-9

Huck, C. W., Guggenbichler, W., & Bonn, G. K. (2005). Analysis of caffeine, theobromine and theophylline in coffee by near infrared spectroscopy (NIRS) compared to high-performance liquid chromatography (HPLC) coupled to mass spectrometry. *Analytica*

© COPYRIGHT UPM

Chimica Acta, *538*(1–2), 195–203. https://doi.org/10.1016/j.aca.2005.01.064

Hughes, J., Izake, E. L., Lott, W. B., Ayoko, G. A., & Sillence, M. (2014). Ultra sensitive label free surface enhanced raman spectroscopy method for the detection of biomolecules. *Talanta*, *130*, 20–25. https://doi.org/10.1016/j.talanta.2014.06.012

Jorgenson, R. C., & Yee, S. S. (1993). A fiber-optic chemical sensor based on surface plasmon resonance. *Sensors and Actuators: B. Chemical*, *12*(3), 213–220. https://doi.org/10.1016/0925-4005(93)80021-3

Kamaruddin, N. H., Bakar, A. A. A., Mobarak, N. N., Dzulkefly Zan, M. S., & Arsad, N. (2017). Binding affinity of a highly sensitive Au/Ag/Au/chitosan-graphene oxide sensor based on direct detection of Pb^{2+} and Hg^{2+} ions. *Sensors (Switzerland)*, *17*(10). https://doi.org/10.3390/s17102277

Kamaruddin, N. H., Bakar, A. A. A., Yaacob, M. H., Mahdi, M. A., Zan, M. S. D., & Shaari, S. (2016). Enhancement of chitosan-graphene oxide SPR sensor with a multi-metallic layers of Au-Ag-Au nanostructure for lead(II) ion detection. *Applied Surface Science*, *361*, 177–184. https://doi.org/10.1016/j.apsusc.2015.11.099

Kant, R., Tabassum, R., & Gupta, B. D. (2017). Integrating nanohybrid membranes of reduced graphene oxide: Chitosan: silica sol gel with fiber optic SPR for caffeine detection. *Nanotechnology*, *28*(19). https://doi.org/10.1088/1361-6528/aa6a9c

Karimian, A., Parsian, H., Majidinia, M., Rahimi, M., Mir, S. M., Samadi Kafil, H., Shafiei-Irannejad, V., Kheyrollah, M., Ostadi, H., & Yousefi, B. (2019). Nanocrystalline cellulose: Preparation, physicochemical properties, and applications in drug delivery systems. *International Journal of Biological Macromolecules*, *133*, 850–859. https://doi.org/10.1016/j.ijbiomac.2019.04.117

© COPYRIGHT UPM

Kim, Y. D., Min, J. Y., Karigar, C. S., Cheong, G. W., Kim, J. W., & Choi, M. S. (2007). Rapid screening and selection of low-caffeine-containing tea (Camellia sinensis) trees by a colorimetric method. *Plant Breeding*, *126*(6), 634–637. https://doi.org/10.1111/j.1439-0523.2006.01349.x

Liedberg, B., Nylander, C., & Lunström, I. (1983). Surface plasmon resonance for gas detection and biosensing. *Sensors and Actuators*, *4*(C), 299–304. https://doi.org/10.1016/0250-6874(83)85036-7

Lin, W. Bin, Jaffrezic-Renault, N., Gagnaire, A., & Gagnaire, H. (2000). Effects of polarization of the incident light-modeling and analysis of a SPR multimode optical fiber sensor. *Sensors and Actuators, A: Physical*, *84*(3), 198–204. https://doi.org/10.1016/S0924-4247(00)00345-9

Luisier, N., Ruggi, A., Steinmann, S. N., Favre, L., Gaeng, N., Corminboeuf, C., & Severin, K. (2012). A ratiometric fluorescence sensor for caffeine. *Organic and Biomolecular Chemistry*, *10*(37), 7487–7490. https://doi.org/10.1039/c2ob26117k

Luque-Pérez, E., Ríos, A., Valcárcel, M., Danielsson, L. G., & Ingman, F. (1999). Spectrophotometric flow injection determination of caffeine in solid and slurry coffee and tea samples using supported liquid membranes. *Laboratory Automation and Information Management*, *34*(2), 131–142. https://doi.org/10.1016/S1381-141X(99)00015-5

Masoum, S., & Heshmat, S. (2015). Photoluminescence quantitative analysis of gallic acid and caffeine in green tea using multi-way chemometric approaches. *Iranian Journal of Mathematical Chemistry*, *6*(2), 109–119. https://doi.org/10.22052/ijmc.2015.10410

Mehrparvar, A., & Rahimpour, A. (2015). Surface modification of novel polyether sulfone amide (PESA) ultrafiltration membranes by grafting hydrophilic monomers. *Journal of Industrial and Engineering Chemistry*, *28*, 359–368.

© COPYRIGHT UPM

https://doi.org/10.1016/j.jiec.2015.03.016

Nanjundaiah, S., Krishna, H., & Bhatt, P. (2016). Fluorescence based turn-on probe for the determination of caffeine using europium-tetracycline as energy transfer complex. *Journal of Fluorescence*, *26*(3), 1115–1121. https://doi.org/10.1007/s10895-016-1803-6

Nemati, F., Hosseini, M., Zare-Dorabei, R., Salehnia, F., & Ganjali, M. R. (2018). Fluorescent turn on sensing of caffeine in food sample based on sulfur-doped carbon quantum dots and optimization of process parameters through response surface methodology. *Sensors and Actuators, B: Chemical*, *273*, 25–34. https://doi.org/10.1016/j.snb.2018.05.163

Nguyen, H. H., Park, J., Kang, S., & Kim, M. (2015). Surface plasmon resonance: A versatile technique for biosensor applications. *Sensors (Switzerland)*, *15*(5), 10481–10510. https://doi.org/10.3390/s150510481

Ogunneye, A. L., Banjoko, O. O., Gbadamosi, M. R., Falegbe, O. H., Moberuagba, K. H., & Badejo, O. A. (2021). Spectrophotometic determination of caffeine and vitamin B6 in selected beverages, energy/soft drinks and herbal products. *Nigerian Journal of Basic and Applied Sciences*, *28*(1), 22–29. https://doi.org/10.4314/njbas.v28i1.4

Omar, N. A. S., Fen, Y. W., Abdullah, J., Chik, C. E. N. C. E., & Mahdi, M. A. (2018). Development of an optical sensor based on surface plasmon resonance phenomenon for diagnosis of dengue virus E-protein. *Sensing and Bio-Sensing Research*, *20*, 16–21. https://doi.org/10.1016/j.sbsr.2018.06.001

Omar, N. A. S., Fen, Y. W., Abdullah, J., Zaid, M. H. M., Daniyal, W. M. E. M. M., & Mahdi, M. A. (2019). Sensitive surface plasmon resonance performance of cadmium sulfide quantum dots-amine functionalized graphene oxide based thin film towards dengue virus E-protein. *Optics and Laser Technology*, *114*, 204–208. https://doi.org/10.1016/j.optlastec.2019.01.038

© COPYRIGHT UPM

Özgür, E., Topçu, A. A., Yılmaz, E., & Denizli, A. (2020). Surface plasmon resonance based biomimetic sensor for urinary tract infections. *Talanta*, *212*, 120778. https://doi.org/10.1016/j.talanta.2020.120778

Ramdzan, N. S. M., Fen, Y. W., Omar, N. A. S., Anas, N. A. A., Daniyal, W. M. E. M. M., Saleviter, S., & Zainudin, A. A. (2019). Optical and surface plasmon resonance sensing properties for chitosan/carboxyl-functionalized graphene quantum dots thin film. *Optik*, *178*, 802–812. https://doi.org/10.1016/j.ijleo.2018.10.071

Rochat, S., Steinmann, S. N., Corminboeuf, C., & Severin, K. (2011). Fluorescence sensing of caffeine in water with polysulfonated pyrenes. *Chemical Communications*, *47*(38), 10584–10586. https://doi.org/10.1039/c1cc13927d

Roche, P. J. R., Ng, S. M., Page, K., Goddard, N., & Narayanaswamy, R. (2009). Surface plasmon resonance sensor in the analysis of caffeine binding to CYP1A2 p450 monoxygenase in the presence and absence of NADPH. *Sensors and Actuators, B: Chemical*, *139*(1), 97–103. https://doi.org/10.1016/j.snb.2008.09.043

Rosddi, N. N. M., Fen, Y. W., Omar, N. A. S., Anas, N. A. A., Hashim, H. S., Ramdzan, N. S. M., Fauzi, N. I. M., Anuar, M. F., & Daniyal, W. M. E. M. M. (2021). Glucose detection by gold modified carboxyl-functionalized graphene quantum dots-based surface plasmon resonance. *Optik*, *239*, 166779. https://doi.org/10.1016/j.ijleo.2021.166779

Saha, S., & Sarkar, P. (2016). Differential pulse anodic stripping voltammetry for detection of As (III) by Chitosan-Fe(OH)$_3$ modified glassy carbon electrode: A new approach towards speciation of arsenic. *Talanta*, *158*, 235–245. https://doi.org/10.1016/j.talanta.2016.05.053

Shehata, M., Azab, S. M., & Fekry, A. M. (2020). Facile caffeine electrochemical detection via electrodeposited Ag nanoparticles with modifier polymers on carbon paste sensor at

© COPYRIGHT UPM

aqueous and micellar media. *Canadian Journal of Chemistry*, *98*(4), 169–178. https://doi.org/10.1139/cjc-2019-0195

Siering, C., Beermann, B., & Waldvogel, S. R. (2006). Supramolecular approach for sensing caffeine by fluorescence. *Supramolecular Chemistry*, *18*(1), 23–27. https://doi.org/10.1080/10610270500310479

Tang, A., & Wang, J. (2020). Manipulating the polymerization of 3,5-diaminobenzoic acid with a bromate oscillator. *Journal of Physical Chemistry C*, *124*(8), 4637–4643. https://doi.org/10.1021/acs.jpcc.0c00323

Thomas, P. S., & Farquhar, M. N. (1978). Specific measurement of DNA in nuclei and nucleic acids using diaminobenzoic acid. *Analytical Biochemistry*, *89*(1), 35–44. https://doi.org/10.1016/0003-2697(78)90724-8

Ummartyotin, S., & Manuspiya, H. (2015). A critical review on cellulose: From fundamental to an approach on sensor technology. *Renewable and Sustainable Energy Reviews*, *41*, 402–412. https://doi.org/10.1016/j.rser.2014.08.050

Vahed, H., & Nadri, C. (2019). Sensitivity enhancement of SPR optical biosensor based on Graphene–MoS2 structure with nanocomposite layer. *Optical Materials*, *88*, 161–166. https://doi.org/10.1016/j.optmat.2018.11.034

Xia, Z., Ni, Y., & Kokot, S. (2013). Simultaneous determination of caffeine, theophylline and theobromine in food samples by a kinetic spectrophotometric method. *Food Chemistry*, *141*(4), 4087–4093. https://doi.org/10.1016/j.foodchem.2013.06.121

Xu, W., & Chang, Y. T. (2016). Quantitative measurement of caffeine by optical methods. *In Neuropathology of Drug Addictions and Substance Misuse* (Vol. 3). Elsevier. https://doi.org/10.1016/B978-0-12-800634-4.00081-0

© COPYRIGHT UPM

Yekta, R., Sadeghi, L., Ahmadi-Kandjani, S., Naziri, P., Rashidi, M.-R., & Dehghan, G. (2021). The impact of caffeine on tau-tau interaction: LSPR detection, structural modification and molecular dynamics simulation. *Journal of Molecular Liquids*, 115914. https://doi.org/10.1016/j.molliq.2021.115914

Zhang, Q. L., Lian, H. Z., Wang, W. H., & Chen, H. Y. (2005). Separation of caffeine and theophylline in poly(dimethylsiloxane) microchannel electrophoresis with electrochemical detection. *Journal of Chromatography A*, *1098*(1–2), 172–176. https://doi.org/10.1016/j.chroma.2005.08.055

Zheng, H., Ni, D., Yu, Z., Liang, P., & Chen, H. (2016). Fabrication of flower-like silver nanostructures for rapid detection of caffeine using surface enhanced Raman spectroscopy. *Sensors and Actuators, B: Chemical*, *231*, 423–430. https://doi.org/10.1016/j.snb.2016.03.045

Zijlstra, P., Paulo, P. M. R., Yu, K., Xu, Q.-H., & Orrit, M. (2012). Chemical interface damping in single gold nanorods and its near elimination by tip-specific functionalization. *Angewandte Chemie*, *124*(33), 8477–8480. https://doi.org/10.1002/ange.201202318

© COPYRIGHT UPM